Journal of Medicinal Chemistry

Article

Dual Targeting of the Adenosine A Receptors and Monoamine Oxidase B by 4*H*-3,1-Benzothiazin-4-ones

Anne Stößel, Sonja Hinz, Petra Küppers, Jag Heer, Michael Gütschow, and Christa E Müller

J. Med. Chem., **Just Accepted Manuscript** • DOI: 10.1021/jm400336x • Publication Date (Web): 30 Apr 2013

Journal of Medicinal Chemistry is published by the American Chemical Society. 1155 Sixteenth Street N.W., Washington, DC 20036

Dual Targeting of Adenosine A_{2A} Receptors and Monoamine Oxidase B by 4*H*-3,1-Benzothiazin-4-ones

Anne Stößel,[§] Sonja Hinz,[§] Petra Küppers,[§] Jag Heer,[†] Michael Gütschow,[§,*] and Christa E. Müller[§,*]

[§]PharmaCenter Bonn, University of Bonn, Pharmaceutical Institute, Pharmaceutical Chemistry I, Bonn, Germany

[†]UCB S.A., Medicinal Chemistry & Lead Generation, CNS Research, Chemin du Foriest, B-1420 Braine l'Alleud, Belgium

ABSTRACT

Blockade of A_{2A} adenosine receptors (A_{2A}ARs) and inhibition of monoamine oxidase B (MAO-B) in brain are considered attractive strategies for the treatment of neurodegenerative diseases such as Parkinson's disease (PD). In the present study benzothiazinones, e.g. 2-(3-chlorophenoxy)-*N*-(4-oxo-4*H*-3,1-benzothiazin-2-yl)acetamide (**13**), were identified as a novel class of potent MAO-B inhibitors (IC_{50} human MAO-B: 1.63 nM). Benzothiazinones with large substituents in the 2-position, e.g. methoxy-cinnamoylamino, phenylbutyrylamino, or chlorobenzylpiperazinylbenzamido residues (**14**, **17**, **27**, **28**) showed high affinity and selectivity for A_{2A}ARs (K_i human A_{2A}AR: 39.5-69.5 nM). By optimizing benzothiazinones for both targets the first potent, dual-acting A_{2A}AR/MAO-B inhibitors with a non-xanthine structure were developed. The best derivative was *N*-(4-oxo-4*H*-3,1-benzothiazin-2-yl)-4-phenylbutanamide (**17**, K_i human A_{2A} 39.5 nM, IC_{50} human MAO-B 34.9 nM; selective versus other AR subtypes and MAO-A), which inhibited A_{2A}AR-induced cAMP accumulation and showed competitive, reversible MAO-B inhibition. The new compounds may be useful tools for validating the A_{2A}AR/MAO-B dual target approach in PD.

KEYWORDS: A_1, A_{2A}, A_{2B}, A_3 antagonists, adenosine receptors, benzothiazinones, dual-acting drugs, MAO-B inhibitors, neurodegenerative disease, Parkinson's disease, structure-activity relationships

INTRODUCTION

Parkinson's disease (PD) is a chronic neurodegenerative disorder of the central nervous system, characterized by the loss of dopaminergic neurons in the substantia nigra and the subsequent depletion of dopamine stores.[1] The consequence is a progressive impairment in motor functions characterized by rigidity, resting tremor and bradykinesia as major symptoms.[1] The current treatment for PD includes the administration of levodopa, a metabolic precursor of dopamine (DA) to increase the DA level, as well as dopamine agonists to mimic the dopamine-mediated neurotransmission. This DA replacing therapy alleviates most of the symptoms especially in the early stage of the disease, but cannot stop the neurodegenerative processes. In particular, a long-term levodopa treatment leads to the development of adverse effects, such as dyskinesia, a disorder characterized by involuntary motor movements. Furthermore, increasing doses are required to maintain the therapeutic effect, and after several years, the drug often loses its effect.[2] For these reasons, the development of novel disease-modifying drugs that stop or at least retard disease progression, delay the onset of levodopa therapy and/or reduce levodopa doses, is urgently needed in PD therapy.[3]

The A_{2A} adenosine receptor (A_{2A}AR), which is activated by the nucleoside adenosine, represents one promising target for anti-Parkinsonian drugs.[1,4] Four subtypes of adenosine receptors (ARs) exist, referred to as A_1, A_{2A}, $A_{2B,}$ and A_3. They belong to the superfamily of G protein-coupled receptors (GPCRs) and differ in their affinity for adenosine, in the type of G proteins that they recruit and in the subsequent downstream signaling pathways that are activated in the target cells.[5] While A_1 and A_3 receptors preferentially inhibit adenylate cyclase (AC) activity and thereby reduce intracellular cAMP production, A_{2A} and A_{2B}ARs stimulate AC and consequently increase cAMP levels. The A_{2A}AR shows a restricted expression in the central nervous system being mainly localized in dopamine-innervated areas, such as the nucleus accumbens, the caudate-putamen, and the olfactory tubercle.[6] The A_{2A}AR is colocalized and physically associated with the dopamine D_2 receptor, forming heteromeric A_{2A}/D_2 receptor complexes.[4,7] Both receptors have an opposing effect on AC and the cellular production of cAMP. Inhibition of A_{2A}ARs leads to enhanced D_2 receptor function and therefore a potentiated

dopamine neurotransmission, while an activation of A_{2A}ARs inhibits D_2 receptor signaling.[8] Thus, binding of agonists to A_{2A}ARs reduces the affinity of DA and other DA agonists for their binding site at the heteromeric DA receptor.[7]

The blockade of the A_{2A}AR is considered as an attractive non-dopaminergic treatment for PD.[1,9] A large number of structurally diverse A_{2A}AR antagonists has been identified to date (for example see Figure 1).[4,10,11] These include xanthine-like structures, e.g. istradefylline (**1**), (*E*)-8-(3-chlorostyryl)caffeine (**2**), and adenine-like compounds, e.g. preladenant (**3**). While **1** is expected to be marketed for the treatment of PD in Japan in the near future, **3** is currently being evaluated in phase III clinical trials, and both drugs have demonstrated beneficial anti-Parkinsonian effects.[4,11] Experimental models of PD indicated that A_{2A} antagonists might be less prone to induce dyskinesias than treatment with levodopa.[11] Furthermore, several animal studies indicated neuroprotective effects induced by a blockade of A_{2A}ARs.[4] Novel A_{2A} antagonists, such as the benzothiazole derivative tozadenant (SYN-115, **4**)[12] and the benzothiazinone **5**,[13] that are structurally neither related to xanthines nor to adenine have been identified by high-throughput screening. Recently, virtual screening approaches have provided further novel scaffolds.[10,14]

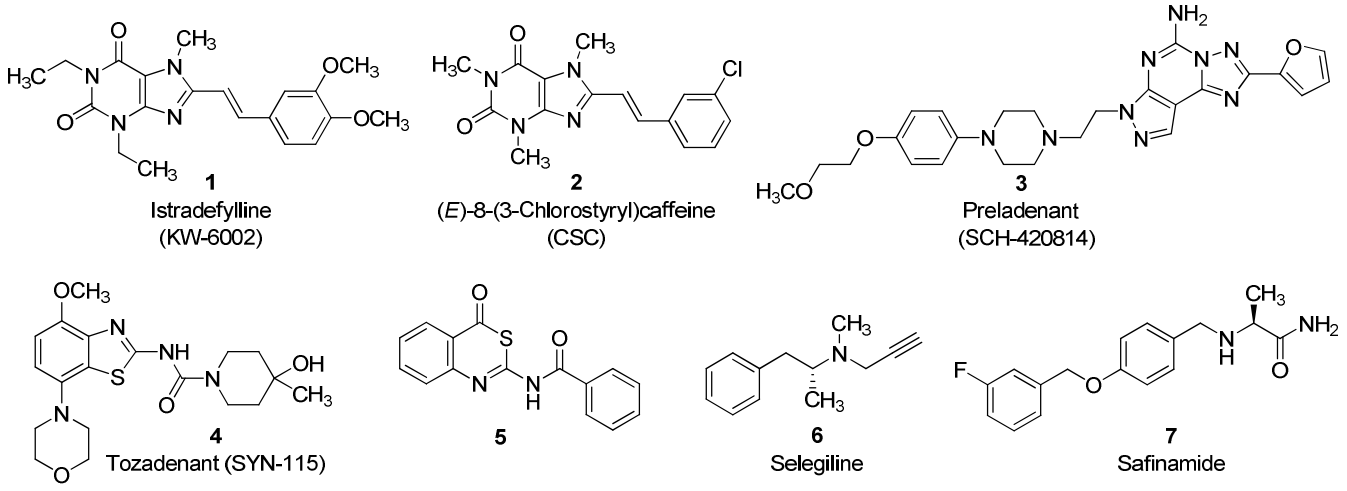

Figure 1. Structures of selected A_{2A} adenosine receptor antagonists (**1**-**5**) and MAO-B inhibitors (**6**, **7**).

Another therapeutic approach in the treatment of PD is provided by the blocking of monoamine oxidase B (MAO-B).[15] This flavin adenine dinucleotide (FAD) containing enzyme is one of the two existing isoforms A and B, which catalyze the oxidative deamination of amine neurotransmitters. Both isoforms

are present in the human brain and involved in the catabolic pathway of dopamine in the striatum.[16] MAO-A is the prevalent isoform in catecholaminergic neurons, whereas MAO-B is predominantly located in glial cells and serotonergic neurons. The activity as well as the expression levels of MAO-B in the human brain increase with age, while MAO-A activity remains constant.[17] Moreover, the increased MAO-B activity, e.g. under levodopa treatment, is associated with a higher production of hydrogen peroxide. The occurrence of reactive oxygen species (ROS) may contribute to apoptotic signaling causing the death of neuronal cells.[18] Inhibition of the enzyme MAO-B improves symptoms of PD. Selegiline (**6**) and the related drug rasagiline are successfully used as irreversible inhibitors in PD monotherapy or in combination with levodopa.[19] For safety reasons and to prevent undesired side effects, reversible inhibitors (e.g. **7**) might be advantageous. Safinamide (**7**) is currently under development in phase III clinical trials as an adjuvant therapy for PD.[20]

Considering these two promising approaches, a compound that antagonizes A_{2A}ARs on the one hand, and inhibits MAO-B on the other hand may have enhanced therapeutic and neuroprotective potential in the treatment of PD. Such drugs would possess the combined benefits of addressing two pharmacological targets with a reduced risk for side effects compared to a combination of two separate drugs.[21] Examples for such an approach include dual-acting drug candidates for neurodegenerative diseases addressing both MAO-B and acetylcholinesterase.[22] Moreover, it has been discovered, that the well known A_{2A} antagonist **2** is also a potent and reversible MAO-B inhibitor.[23] A series of analogues of **2** has been developed in the course of the continued exploration of the dual targeting concept.[24] One major drawback of xanthines, such as compound **2**, is their low water solubility.[25,26] Furthermore, all recently published dual compounds blocking A_{2A}ARs and MAO-B are styryl- or phenylbutadienyl-substituted xanthine derivatives, which are not only highly lipophilic, but in addition sensitive to light, undergoing light-induced isomerization in solution, or light-induced dimerization in the solid state, respectively.[27]

In the present study we focused on the development of non-xanthine-derived, dual-acting compounds, which exhibit an antagonistic effect at A_{2A}ARs and at the same time inhibit MAO-B. Previously

reported 4*H*-3,1-benzothiazin-4-ones, such as derivative **5**, are potent A_{2A}AR antagonists but lack selectivity versus the other AR subtypes.[13] As a continuation of our research, further 4*H*-3,1-benzothiazin-4-one derivatives have been synthesized and evaluated at all four AR subtypes as well as MAO-B, and optimized for dual A_{2A}/MAO-B blockade.

RESULTS AND DISCUSSION

Chemistry. Scheme 1 outlines the synthetic route towards 4*H*-3,1-benzothiazin-4-ones **8**-**24**. Starting with compound **8**, it was intended to systematically vary and extend the spacer between the heterobicyclic core and the phenyl group and to introduce substituents at the latter. The thioureide **38**, obtained by the reaction of anthranilic acid (**37**) and benzoyl isothiocyanate, gave the benzothiazinone skeleton of **39** in a sulfuric acid-promoted cyclization with a concomitant loss of the benzoyl residue.[28] Structural diversity of **8**-**24** was introduced in the last step of this route by an acylation reaction according to a previously described procedure.[13] Because of the low nucleophilicity of the amino group of **39**, several carboxylic acids (**40** and **41**) were activated as mixed anhydrides using the Yamaguchi reagent (2,4,6-trichlorobenzoyl chloride).[13]

Scheme 1. Synthesis of 2-Acylaminobenzothiazinones **8**-**24**[a]

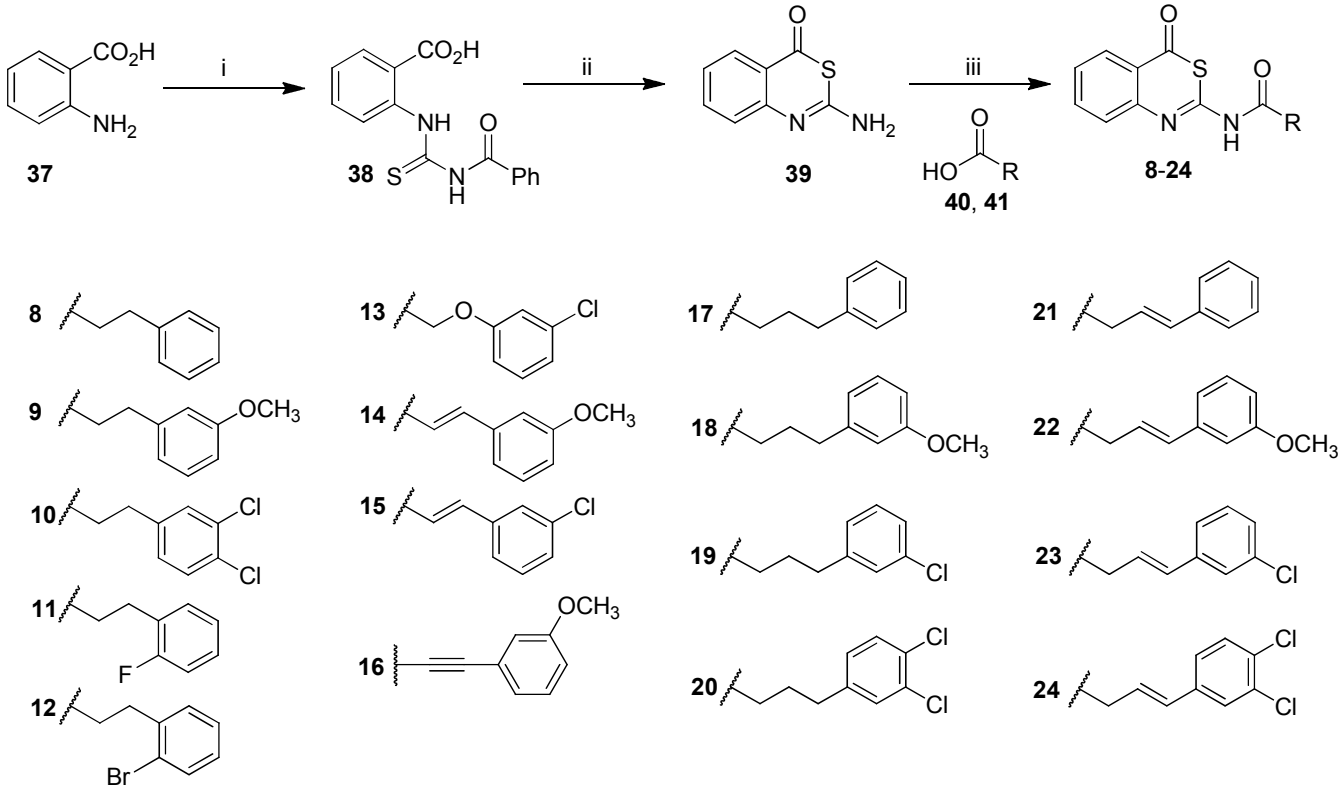

[a]Reagents and conditions: (i) benzoyl isothiocyanate, acetone, RT, 20 min; (ii) 1. concd H_2SO_4, 100 °C, 4 h, 2. $NaHCO_3$; (iii) 1. carboxylic acids **40** or **41** (residues R correspond to those of compounds **8**-**24**), *N*-methylmorpholine, 2,4,6-trichlorobenzoyl chloride, THF, RT, 1 h, 2. **39**, pyridine, toluene, reflux, 2 h.

Some of the required carboxylic acids **40** and **41** are expensive or not commercially available and were prepared as follows. The phenylbutenoic acid derivatives **40** were obtained via a Wittig reaction (Scheme 2), and for this purpose, the phosphonium salt of 3-bromopropionic acid (**42**) was generated and reacted with the appropriate aldehydes **43** to form the alkenes **40**.

Scheme 2. Synthesis of Phenylbutenoic Acids **40** and Phenylbutyric Acids **41**[a]

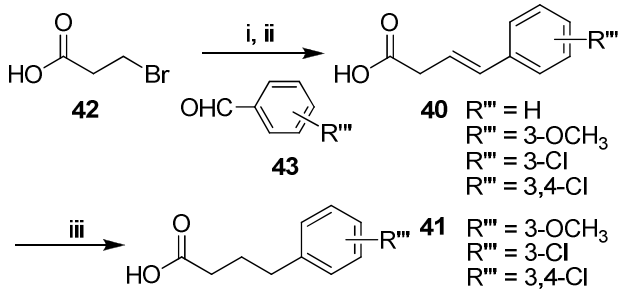

[a]Reagents and conditions: (i) PPh_3, acetonitrile, reflux, 5 h; (ii) 1. aldehyde **43**, *tert*-BuOK, CH_2Cl_2, 0 °C → RT, 12 h; (iii) Pd/C, H_2, EtOH or THF, RT, 1-2 h.

A subsequent Pd-catalyzed hydrogenation step provided the saturated phenylbutyric acids **41**. 3-(2-Fluorophenyl)propanoic acid (see Scheme 1) was similarly obtained via hydrogenation of the corresponding cinnamic acid. 3-(3-Methoxyphenyl)propiolic acid was synthesized according to a literature procedure.[29]

In order to increase the compounds' polarity and water solubility, we planned to attach a basic moiety. Previous studies indicated an *N*-benzylpiperazine residue connected via an amide bond to the benzoylaminobenzothiazinone as in compound **25**[13] (Scheme 3) to be an advantageous substitution pattern with respect to bioactivity and solubility.[13]

Scheme 3. Synthesis of 2-Acylaminobenzothiazinones **26-28**[a]

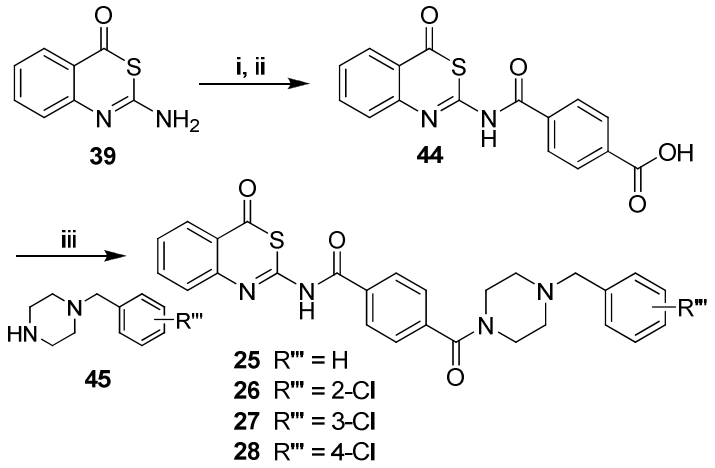

[a]Reagents and conditions: (i) 1. 4-formylbenzoic acid, $(COCl)_2$, DMF (cat), CH_2Cl_2, RT, 2 h, 2. pyridine, CH_2Cl_2, reflux, 2 h; (ii) oxone, DMF, RT, 12 h; (iii) 1. 1,1'-carbonyldiimidazole, DMF, RT, 1 h, 2. piperazine **45** (1.25 equiv), imidazole (1.0 equiv), HCl (2.0 equiv), DMF, RT, 2 h.

To synthesize further analogues, 4-formylbenzoic acid was activated by the conversion to the acyl chloride and reacted with 2-aminobenzothiazinone **39**. According to a reported method,[30] oxone was successfully utilized to oxidize the intermediate aldehyde to the corresponding carboxylic acid **44**. In order to prevent a Dimroth rearrangement of the benzothiazinone system,[31] an imidazole buffer was applied for the carbonyldiimidazole-promoted coupling of **43** with different *N*-benzylpiperazines **45** to give the basic carboxamides **26-28**. The following syntheses were performed in order to achieve minor structural modifications of compound **17** (Scheme 1) as this benzothiazinone turned out to be a particular promising candidate (see afterwards).

Scheme 4. Synthesis of *N*-Methylated 2-Acylaminobenzothiazinone **29**[a]

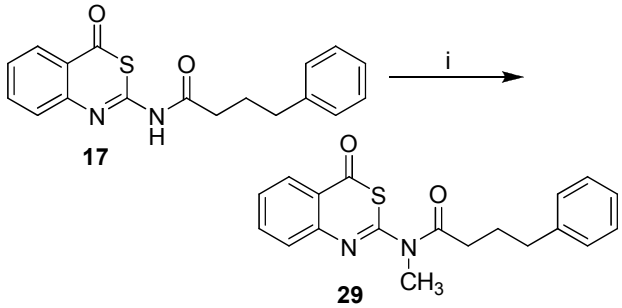

[a]Reagents and conditions: (i) 1. CH_3I, THF, 0 °C, 2. NaH, RT, 24 h.

To identify the potential role of the amide proton as a hydrogen bond donor for protein binding, the *N*-methylated compound **29** was prepared (Scheme 4).

Scheme 5. Synthesis of Substituted 2-Acylaminobenzothiazinones **30-33** and 2-Acylaminothienothiazinone **34-36**[a]

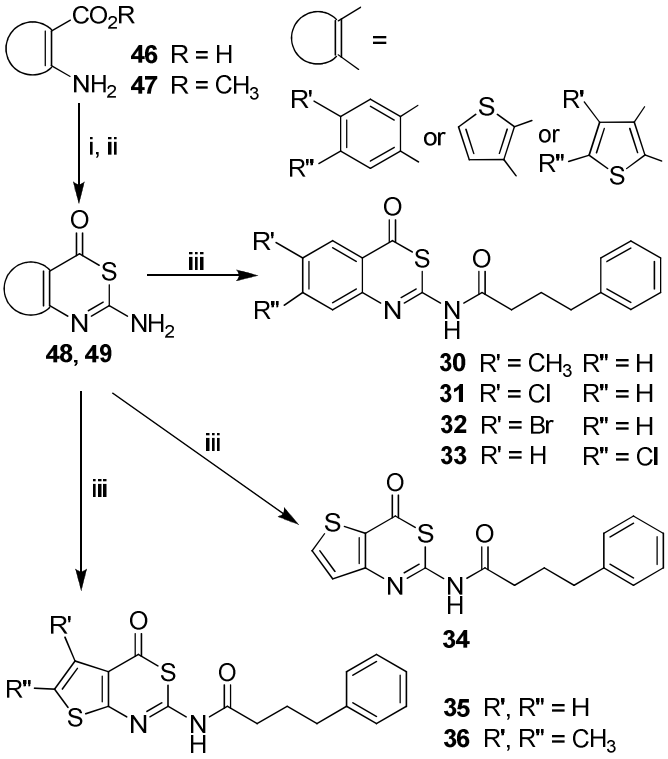

[a]Reagents and conditions: (i) benzoyl isothiocyanate, acetone, RT, 20 min; (ii) 1. concd H_2SO_4, 100 °C, 4 h, 2. $NaHCO_3$; (iii) 1. 4-phenylbutyric acid, *N*-methylmorpholine, 2,4,6-trichlorobenzoyl chloride, THF, RT, 2. amine **48** or **49**, pyridine, toluene, reflux, 2 h.

Substituted 2-amino-4*H*-3,1-benzothiazin-4-ones **30-33** were synthesized (Scheme 5) in order to implement diversity at the fused benzene ring. Additionally, a bioisosteric replacement by a non- or dimethyl-substituted thiophene moiety (compounds **34-36**) increases the electron density of the thiazinone ring, which may have an impact on its interaction with the target proteins. In all derivatives the acyl residue of compound **17** was kept constant. The starting reaction was carried out under the conditions specified in Scheme 1 to yield derivatives **48** and **49**, whose acylation with 4-phenylbutyric acid resulted in the target compounds **30-36**.

Radioligand Binding Studies at Adenosine Receptors. The newly synthesized derivatives (**8-36**) were investigated in radioligand binding studies, in most cases initially at rat brain A_1 and A_{2A}ARs and in

case of measurable affinities subsequently at human recombinant A_1, A_{2A}, A_{2B} and A_3ARs expressed in Chinese hamster ovary (CHO) cells.[32] For binding assays at A_1ARs, [^{3}H]2-chloro-*N*^{6}-cyclopentyladenosine (CCPA) and at A_{2A} receptors, [^{3}H]3-(3-hydroxypropyl)-7-methyl-8-(*m*-methoxystyryl)-1-propargylxanthine (MSX-2) were used as selective radioligands in both species. For A_{2B}AR binding studies, the selective radioligand [^{3}H]8-(4-(4-(4-chlorophenyl)piperazine-1-sulfonyl)phenyl)-1-propylxanthine (PSB-603) and for A_3AR binding studies, the A_3-selective radioligand [^{3}H]2-phenyl-8-ethyl-4-methyl-(8*R*)-4,5,7,8-tetrahydro-1*H*-imidazo[2,1-*i*]purin-5-one (PSB-11) were employed. Initial screening was usually performed at two concentrations, 10 μM and 1 μM. In A_{2B} and A_3 radioligand binding studies, the highest concentration of test compound was 1 μM because higher concentrations often led to precipitation of the radioligands [^{3}H]PSB-603 and [^{3}H]PSB-11. The results of the AR binding assays are presented in Table 1 together with data for standard ligands for comparison.

Table 1. Adenosine Receptor Affinities of **1-36**.

2-Acylaminobenzothiazinones		Substituted 2-acylaminobenzothiazinones and 2-acylaminothienothiazinones			
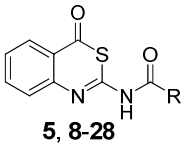 **5**, **8-28** for R see below	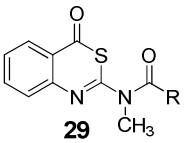 **29**	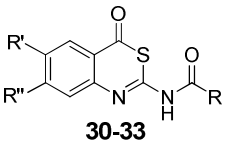 **30-33**	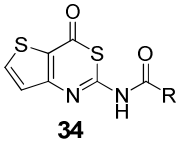 **34**	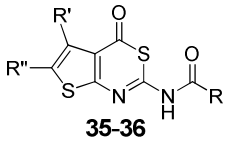 **35-36**	**29-36** R = $(CH_2)_3Ph$

compd		K_i ± SEM (nM)[a]					
		rat A_1 vs. [^{3}H]CCPA	**rat A_{2A}** vs. [^{3}H]MSX-2	**human A_1** vs. [^{3}H]CCPA	**human A_{2A}** vs. [^{3}H]MSX-2	**human A_{2B}** vs [^{3}H]PSB-603	**human A_3** vs [^{3}H]PSB-11
1		230	2.2[b]	841 2830[c]	91.2 36[c]	>10000 >1800[c]	4470 >3000[c]
2		>10000 28000[d]	28.1 ± 5.5 28[e]	>10000	38.1 ± 12.7 30[e]	>1000 8200[d]	>1000
3		68.7 ± 8.7	0.66 ± 0.12	295 ± 10	0.884 ± 0.32	>1000	>1000
thiazinones 5, 8-29							
	R						
5[f]		25 ± 5	609 ± 61	309 ± 17	91.7 ± 16.9	360 ± 100	30.4 ± 6.8
8	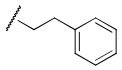	422 ± 75	103 ± 10	1050 ± 161	80.9 ± 21.3	365 ± 63	390 ± 69
9	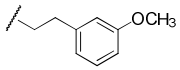	367 ± 16	294 ± 137	1370 ± 195	64.9 ± 12.4	225 ± 33	173 ± 18
10	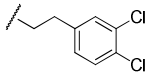	>1500	>10000	n.d.[g]	n.d.	>1000[h]	>1000[h]
11	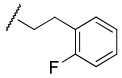	>10000	2190 ± 863	n.d.	n.d.	801 ± 139	≥1000[h]
12	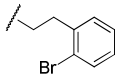	>10000	>10000	n.d.	n.d.	>1000[h]	>1000[h]
13	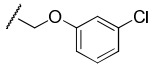	>10000	>10000	n.d.	n.d.	>1000[h]	>1000[h]
14	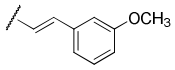	205 ± 19	253 ± 37	>10000[h]	62.4 ± 12.6	679 ± 88	>1000[h]
15	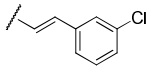	≥10000	>10000	n.d.	>1000	>1000[h]	>1000[h]
16	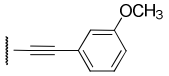	>10000	1720 ± 694	n.d.	≥1000	>1000[h]	>1000[h]
17	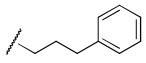	229 ± 103	423 ± 76	2500 ± 660	39.5 ± 5.8	>1000[h]	>1000[h]
18	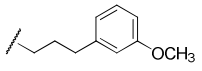	22.5 ± 2.3	558 ± 67	214 ± 11	115 ± 24	302 ± 30	382 ± 106
19	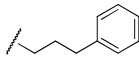	898 ± 253	>10000	>10000	n.d.	≥1000[h]	>1000[h]
20	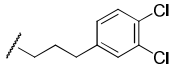	>1500	>10000	n.d.	n.d.	>1000[h]	>1000[h]
21	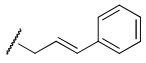	53.0 ± 14.5	814 ± 167	822 ± 146	118 ± 38	119 ± 23	158 ± 45
22	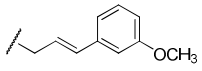	11.2 ± 1.5	317 ± 43	500 ± 59	91.8 ± 25.9	≥1000[h]	115 ± 26
23	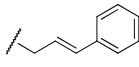	11.4 ± 1.3	≥10000	562 ± 96	n.d.	>1000[h]	>1000[h]

24	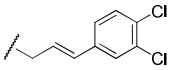	≥1500	>1000	n.d.	n.d.	>1000[h]	>1000[h]
25[f]	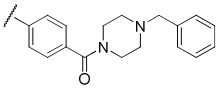	>1000	285 ± 38	>10000	69.5 ± 14.1	178 ± 41	>1000
26	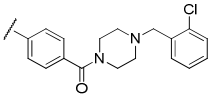	n.d.	>10000	>1000	>1000	>1000	>1000
27	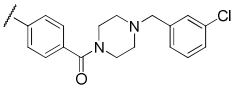	n.d.	84.7 ± 9.8	>1000	58.3 ± 7.6	>1000	>1000
28	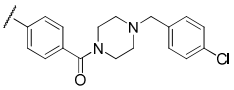	n.d.	488 ± 205	4370 ± 1810	44.3 ± 15.9	>1000[h]	>1000
29	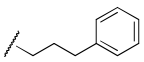	>10000	>10000	n.d.	>10000	>1000[h]	>1000[h]
thiazinones 30-36							
	R'	R''					
30	CH_3	H	98.3 ± 48.0	6060 ± 1940	>1000	n.d.	408 ± 31	147 ± 55
31	Cl	H	>10000	>10000	n.d.	n.d.	>1000[h]	>1000[h]
32	Br	H	>10000	>10000	n.d.	n.d.	>1000[h]	>1000[h]
33	H	Cl	64.4 ± 22.9	≥10000	785 ± 339	n.d.	>1000[h]	91.6 ± 14.1
34	-	-	≥10000	>10000	n.d.	n.d.	547 ± 167	>1000[h]
35	H	H	35.2 ± 1.2	693 ± 141	364 ± 184	82.5 ± 29.5	361 ± 88	>1000[h]
36	CH_3	CH_3	>10000	>10000	n.d.	n.d.	>1000[h]	>1000[h]

[a]n = 3, unless otherwise noted. [b]Data from ref. 33. [c]Data from ref. 34. [d]Data from ref. 35. [e]Data from ref. 24b. [f]Data from ref. 13. [g]n.d., not determined. [h]n = 2.

Structure-Activity Relationships at Adenosine Receptors. The phenylpropionyl derivative **8** was potent at the human A_{2A}AR (K_i = 80.9 nM) and showed a higher selectivity over the human A_1 and A_3AR subtypes than the previously described homolog, the benzoyl derivative compound **5**. For the purpose of further optimization, a first set of related derivatives (**9-24**), characterized by different acyl residues at the exocyclic 2-amino group, was synthesized. The introduction of a methoxy group in the 3-position of the phenyl ring (compound **9**) was well tolerated by the A_{2A}AR. In contrast to **8**, the affinity for the human subtype (K_i = 64.9 nM) was more than 4-fold higher compared to the rat A_{2A}AR (K_i = 294 nM). The additional 3-methoxy substituent did not improve AR subtype selectivity. A 3,4-dichloro- (compound **10**) as well as a fluoro- or a bromo-substitution in the *ortho*-position (compounds **11** and **12**) greatly reduced or abolished A_{2A} affinity. These halogen-substituted derivatives showed also no or only weak affinity for the other AR subtypes. Only derivative **11** was moderately potent at the A_{2B}AR (K_i =

801 nM). For compound **13**, which contains an aryl ether linkage, no significant affinity for the ARs was observed. Replacement of the 3-(3-methoxyphenyl)propionyl residue of compound **9** by a corresponding cinnamoyl moiety (compound **14**) led to a similarly high A_{2A} affinity (K_i = 62.4 nM). Moreover, the double bond was beneficial concerning selectivity for the human A_{2A}AR, which was 10-fold over the human A_{2B}AR and more than 16-fold versus the A_3AR. While compound **14** was inactive at human A_1AR, it showed good affinity for the rat A_1AR (K_i = 205 nM). An exchange of the methoxy group of **14** for a chloro substituent (compound **15**), or the alkenyl for an alkynyl spacer (compound **16**), respectively, resulted in a loss of affinity.

The extension of the 3-phenylpropionyl- (compound **8**) to a 4-phenylbutyryl-substituent (compound **17**) increased the affinity for the human A_{2A}AR (K_i = 39.5 nM) and provided the best A_{2A} antagonist of the present series. In addition, this spacer elongation had a positive effect on selectivity, which was more than 60-fold over the human A_1 and more than 25-fold over the human A_{2B} and A_3ARs. In contrast, an unsaturated spacer, as in derivative **21**, decreased the A_{2A} affinity 3-fold at human and 2-fold at rat A_{2A}ARs, while increasing affinity for the other three AR subtypes. Introduction of a 3-methoxy substituent at the phenyl ring of **17** leading to compound **18** also reduced the affinity for A_{2A}ARs (hA_{2A}: K_i = 115 nM) and increased A_1, A_{2B} and A_3AR affinities. Similar receptor affinities were obtained for the corresponding 3-methoxy-substituted unsaturated derivative **22**, in which both modifications were combined. In the set of compounds containing one or two chloro substituents at the phenyl ring (**19**, **20**, **23**, and **24**), a complete loss of A_{2A} affinity was observed. These derivatives were also inactive at the other AR subtypes, except for compound **23**, which showed high affinity for the rat A_1AR (K_i = 11.4 nM) and moderate affinity for the human A_1AR (K_i = 562 nM). Among the benzothiazinones bearing a spacer-connected phenyl ring attached to the 2-position of the benzothiazinone core structure (i.e. **8**-**24**), only 3-methoxy-substituted, or unsubstituted derivatives possessed good A_{2A} affinity, whereas halogen-substituted compounds proved to be inactive.

As mentioned above, benzylpiperazine-substituted derivatives **26**-**28** were synthesized to enhance water solubility. Their structure was designed based on the previously reported benzothiazinone derivative

25.[13] Compound **25** with an unsubstituted benzyl residue was found to be a potent A_{2A} and A_{2B} receptor antagonist (hA_{2A}: K_i = 69.5 nM; A_{2B}: K_i = 178 nM) and exhibited high A_{2A}-selectivity versus A_1ARs. Apparently, a chloro substituent (compound **26**) in the *ortho*-position was not tolerated by any of the AR subtypes. In contrast, the A_{2A} affinity of the *meta*- and the *para*-chloro-substituted compounds (hA_{2A}, **27**: K_i = 58.3 nM; **28**: K_i = 44.3 nM) was at least as high as that of the unsubstituted derivative **25**. Moreover, **28** was more than 22-fold selective for A_{2A} versus the A_{2B} and the A_3ARs and nearly 100-fold versus the A_1ARs (human species). These results indicated that the binding pocket for the A_{2A}AR is able to accommodate large and basic substituents and requires a correct orientation of the chloro substituent. Thus, *N*-(chlorobenzyl)piperazine-substituted benzothiazinone derivatives like **27** and **28** are interesting new starting points for the development of selective A_{2A}AR antagonists with an expected improved water solubility, at least in slightly acidic media.

Because of the high A_{2A}AR affinity and selectivity of compound **17**, we used the phenylbutyryl residue as a fixed motif for further modification of the benzothiazinone core and the amide linker (compound **29-36**). Compound **29**, an *N*-methylated derivative of **17**, was completely inactive at all adenosine receptor subtypes. This indicates that the amide proton may be required as a hydrogen bond donor for receptor binding.

Next, we considered the modification of the benzothiazinone core (**30-36**). Neither methyl-, chloro-, or bromo-substitution in the 6-postition, nor a chloro-substituent in the 7-position was tolerated by the rat A_{2A}AR. Finally, the fused benzene ring of **17** was bioisosterically replaced by thiophene (compounds **34-36**). The thieno[3,2-*d*][1,3]thiazin-4-one **34** was inactive at A_1, A_{2A}, and A_3ARs and had only a moderate potency at the A_{2B}AR subtype (K_i = 547 nM). In contrast, the isomeric thieno[2,3-*d*][1,3]thiazin-4-one **35** exhibited high affinities for most of the AR subtypes, except for the A_3AR, comparable to those of the corresponding benzothiazinone analogue **17**. Surprisingly the dimethylated thienothiazinone **36** did not bind to any of the four AR subtypes.

In summary, the benzothiazinones with a methoxy-substituted cinnamoyl or a phenylbutyryl residue (**14**, **17**), as well as representatives with an *N*-(chlorobenzyl)piperazine moiety (**27**, **28**) exhibited the

most favorable properties with regard to A_{2A} affinity and selectivity, being comparable to the standard ligands **1** and **2**.

With respect to bioactivity, the benzothiazinone scaffold turned out to be versatile. We did not only obtain potent A_{2A}AR antagonists, as intended in this study, but also discovered benzothiazinones with high affinity for A_1, A_{2B} and A_3ARs, e.g. **33**, a relatively potent and selective A_3 antagonist for human A_3ARs (K_i = 91.6 nM).

With the exception of **8**, which was equipotent at human and rat A_{2A}ARs, the affinity for the human A_{2A}AR was consistently higher (2-10-fold) than for the rat orthologue (plot of 12 rat pK_i values versus human pK_i values, linear regression, gave the following results: slope = 0.60, y-intercept = 2.16, r^2 = 0.08; for details see Supporting Information). In contrast, all investigated benzothiazinones exhibited lower affinity for the human than for the rat A_1AR (plot of 10 rat pK_i values versus human pK_i values yielded the following results: slope = 1.39, y-intercept = -1.32, r^2 = 0.58; for details see Supporting Information). At that receptor subtype, some derivatives (e.g. **22** and **23**) had a preference for the rat species of up to 45-fold. Such extreme species differences have to be taken into account prior to preclinical in vivo studies, which are typically performed in rodents. In view of the low r^2 values of our analysis, cross-species extrapolations for benzothiazinones are very limited.

Functional Studies at Adenosine Receptors. Cyclic AMP (cAMP) accumulation studies at human A_{2A}ARs were performed with the most potent A_{2A}AR antagonist of the present series, compound **17,** as a representative of the benzothiazinone scaffold (Figure 2).

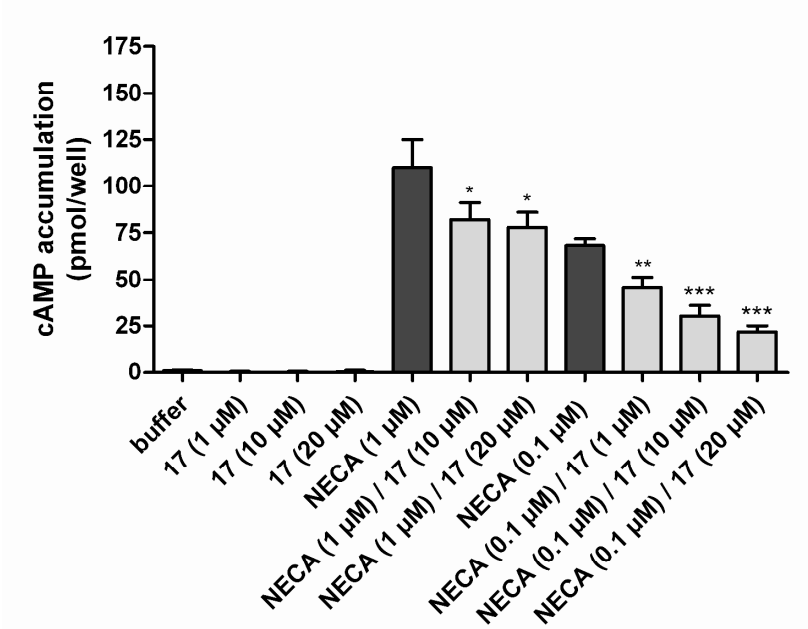

Figure 2. cAMP accumulation experiments in CHO cells stably transfected with the human A_{2A}AR. The non-selective AR agonist NECA (0.1 and 1 µM) showed a concentration-dependent stimulation of cAMP formation. Benzothiazinone **17** did not show an effect by itself but inhibited NECA-induced cAMP accumulation. Graph bars represent results from three independent experiments ± SEM.

Benzothiazinone **17** did not show any agonistic activity at CHO cells transfected with the human A_{2A}AR, even at high concentrations up to 20 µM. However, the increase in intracellular cAMP production induced by the agonist NECA was significantly blocked in the presence of the compound **17**. We used relatively high concentrations of the agonist NECA, and therefore also had to add high concentrations of the antagonist **17** to prove significant inhibitory effects (see Figure 2). These results clearly confirm previous findings that the class of benzothiazinones acts as antagonists at ARs.[13]

Monoamine Oxidase Inhibition Studies. All compounds were investigated for inhibition of rat and human MAO-B using mitochondria-enriched rat liver fractions, and human recombinant MAO-B enzyme, respectively. The commercially available Amplex Red monoamine oxidase assay kit was utilized. MAO-A (human) inhibition assays were performed analogously for selected compounds. The

inhibitors clorgyline for MAO-A and selegiline for MAO-B were used to block the respective enzyme in rat liver fractions for determining selective inhibition of one of the isoenzymes. The inhibitory potencies for the benzothiazinones and for standard inhibitors are collected in Table 2 and 3.

Table 2. MAO-B Inhibitory Potencies of Benzothiazinones and Standard Compounds.

	IC_{50} ± SEM (nM)[a]			IC_{50} ± SEM (nM)[a]	
compd	**rat MAO-B**	**human MAO-B**	**compd**	**rat MAO-B**	**human MAO-B**
2	38.5 ± 5.1	18.1 ± 3.3 96 (baboon enzyme)[b]	**20**	3300 ± 280	3440 ± 1400
			21	361 ± 38	39.8 ± 6.4
6	6.74 ± 0.81, 7[d]	6.13 ± 0.85, 20[d]	**22**	2020 ± 580	238 ± 12
7	25.8 ± 3.0	7.67 ± 1.81	**23**	840 ± 135	>1000
5	>10000	n.d.[e]	**24**	4640 ± 436	>10000
8	42.7 ± 19.8	17.6 ± 3.7	**25**	n.d.	>10000
9	621 ± 39	95.3 ± 8.8	**26**	n.d.	>10000
10	>10000	>10000	**27**	n.d.	>10000
11	725 ± 183	11.2 ± 2.4	**28**	n.d.	>10000
12	64.0 ± 18.4	2.09 ± 0.17	**29**	n.d.	53.1 ± 16.5
13	661 ± 126	1.63 ± 0.18	**30**	325 ± 28[f]	94.0 ± 8.3
14	281 ± 178[f]	470 ± 112	**31**	>10000	>10000
15	815 ± 436	93.3 ± 9.2	**32**	>10000	>10000
16	73.9 ± 16.1	43.7 ± 4.2	**33**	1220 ± 452	76.4 ± 14.7
17	186 ± 37	34.9 ± 2.5	**34**	298 ± 8[f]	206 ± 42
18	1300 ± 80	389 ± 122	**35**	291 ± 107[f]	69.7 ± 6.1
19	6880 ± 310	>1000	**36**	26.6 ± 10.1[f]	9.80 ± 1.97

[a]n = 3, unless otherwise noted. [b]Data from ref. 24b. [c]Data from ref. 36. [d]Data from ref. 37. [e]n.d., not determined. [f]n = 2.

Structure-Activity Relationships at Monoamine Oxidase B. The previously reported benzoyl-substituted 2-aminobenzothiazinone **5**[13] did not show noticeable activity at rat MAO-B. However, extension of the linker to obtain the phenylpropionyl derivative **8** provided the first potent MAO-B inhibitor. Compound **8** exhibited a slight preference for the human versus the rat isoenzyme (human: IC_{50} = 17.6 nM; rat: IC_{50} = 42.7 nM). We therefore considered **8** as a starting point and focused on structural variations to explore the potency of this type of inhibitor more precisely. The introduction of a 3-methoxy group at the phenyl ring (compound **9**) led to decreased inhibition (human: IC_{50} = 95.3 nM; rat: IC_{50} = 621 nM). While a 3,4-dichloro substitution pattern (compound **10**) produced no activity at all,

an *ortho*-fluoro or *ortho*-bromo substitution resulted in potent MAO-B inhibitors at the human enzyme (**11**: IC_{50} = 11.2 nM; **12**: IC_{50} = 2.09 nM). The number and position of halogen substituents on the phenyl ring appeared to be crucial for inhibitory activity towards MAO-B. At the rat enzyme, both compounds were considerably weaker (**11**: IC_{50} = 725 nM, 65-fold; **12**: IC_{50} = 64.0 nM, 31-fold). An incorporation of oxygen into the spacer, and the introduction of a 3-chloro substituent (compound **13**) provided the most potent inhibitor of the entire series (human: IC_{50} = 1.63 nM) and exhibited a nearly 4-fold higher inhibitory activity towards human MAO-B than the irreversible standard inhibitor **6**. Again, **13** was much less potent at the rat MAO-B enzyme (IC_{50} = 661 nM, 400-fold) than at the human ortholog. The high potency of compounds **11**-**13** shows that benzothiazinones represent a new class of potent MAO-B inhibitors. However, all three compounds were inactive at the A_{2A}AR (see above) and therefore not suitable for a dual target approach.

Among the derivatives with an unsaturated spacer (**14-16**), the 3-methoxy-cinnamoyl derivative **14** showed only a moderate effect, and was about equipotent at both species (human: IC_{50} = 470 nM; rat: IC_{50} = 281 nM). The corresponding 3-chlorinated compound **15** was 5-times more potent than the related methoxy derivative **14** only at the human enzyme (human: IC_{50} = 93.3 nM; rat: IC_{50} = 815 nM). Introduction of a (3-methoxyphenyl)propioloyl residue (compound **16**) resulted in a good MAO-B inhibitory potency (human: IC_{50} = 43.7 nM; rat: IC_{50} = 73.9 nM) without species preference.

In the group with an extended spacer (**17-20**), the phenylbutyryl-substituted compound **17** exhibited a remarkable MAO-B inhibitory activity (human: IC_{50} = 34.9 nM; rat: IC_{50} = 186 nM). As noted above, **17** was identified as a potent and selective A_{2A} antagonist and can thus be considered to be a promising dual-acting candidate. The activity of compound **18** with an additional *meta*-methoxy group was about 10-fold lower (human: IC_{50} = 389 nM) compared to the unsubstituted analogue **17**. One or two chloro substituents (**19**, **20**) dramatically decreased the affinity. The same trend was observed for the unsaturated analogs (**21-24**), where only the unsubstituted derivative **21** showed notable MAO-B inhibitory potency (human: IC_{50} = 39.8 nM; rat: IC_{50} = 361 nM). The introduction of different *N*-benzylpiperazine moieties (**25-28**) was not tolerated by MAO-B and resulted in completely inactive

compounds. The activity of the *N*-methylated compound **29** for human MAO-B was only slightly decreased (IC_{50} = 53.1 nM) compared to the corresponding *N*-unsubstituted derivative **17**. This indicates that the amide proton, in contrast to the situation at the $A_{2A}AR$, is not essential for MAO-B binding.

Next, modified 6- or 7-substituted benzothiazinones (**30-33**) and thiophene analogues (**34-36**) were considered. In position 6, only a methyl group (compound **30**) was tolerated by MAO-B (human: IC_{50} = 94.0 nM) whereas the derivatives with a 6-chloro or a 6-bromo substituent (**31** and **32**) were inactive. In contrast, the 7-chlorinated compound **33** was potent towards MAO-B (human: IC_{50} = 76.4 nM). The thieno[3,2-*d*][1,3]thiazin-4-one **34** had a moderate inhibitory effect (human: IC_{50} = 206 nM; rat: IC_{50} = 298 nM) and showed, as one of only a few examples in this series, no major species differences. The isomeric thieno[2,3-*d*][1,3]thiazin-4-one **35** exhibited slightly better MAO-B inhibition (human: IC_{50} = 69.7 nM; rat: IC_{50} = 291 nM) but was still weaker than the benzothiazinone lead structure **17**. Dimethylation of **35** to compound **36** increased potency at both, human and rat MAO-B, leading to a potent MAO-B inhibitor (human: IC_{50} = 9.80 nM; rat: IC_{50} = 26.6 nM) that had a 3-fold higher potency than the lead compound **17**.

Considering the whole series (**8-36**), more than half of the compounds were found to be active at MAO-B. The highest inhibition potencies were achieved with the dimethylated thienothiazinone derivative **36** and benzothiazinones bearing an *ortho*-halogen-substituted phenylpropionyl residue (compound **11** and **12**) or a *meta*-chloro-substituted phenoxyethyl moiety (compound **13**). All of these compounds inhibited MAO-B in the low nanomolar range, comparable or even superior to the standard inhibitors (**6** and **7**). For the established inhibitor **2** as well as related xanthine derivatives and analogues, the styryl moiety had been identified as an essential unit to achieve MAO-B inhibition.[23,24] However, in the present study we could not observe a marked difference between benzothiazinones with a saturated and those with an unsaturated spacer.

A comparison of the IC_{50} values determined at the human and the rat MAO-B enzyme revealed significant species differences. For the present benzothiazinone series (except for **14**, **20**, and **24**) the inhibitory potency at the human MAO-B was always higher (1.4-400-fold) than at the rat enzyme (plot

of 18 rat pIC_{50} values versus human pIC_{50} values, linear regression gave the following results: slope = 0.40, y-intercept = 3.54, $r^2 = 0.33$; for details see Supporting Information). As these differences did not follow a clear trend with respect to the benzothiazinones' structures, it will always be required to determine both, human and rat enzyme inhibition constants, prior to planning preclinical and clinical in vivo studies. Similar findings of moderate correlations between human and rat IC_{50} values were previously reported for other classes of MAO-B inhibitors.[38]

Mechanism of Monoamine Oxidase B Inhibition. It has already been mentioned that, from a therapeutic point of view, reversible inhibition of MAO-B may have significant advantages over the irreversible inactivation of the enzyme. Therefore, it was investigated whether four selected compounds, **8**, **9**, **17**, and **35**, act as reversible or irreversible inhibitors of MAO-B. For this purpose, human MAO-B was treated with a test compound or with the irreversible inhibitor **6**, or the reversible inhibitor **7** as reference compounds, respectively (Figure 3).

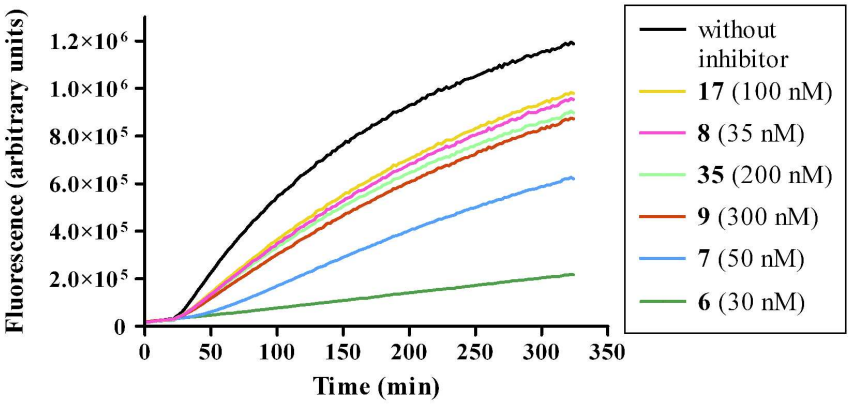

Figure 3. Reactivation of MAO-B. Human MAO-B was treated under assay conditions with several inhibitors (each at the concentration that represents its IC_{80} value) in the presence of the substrate *p*-tyramine. After 22 min, the substrate concentration was increased from 150 µM to 1 mM, and fluorescence was measured over a period of 5 h.

After preincubation, the substrate concentration was increased and the course of the reaction was observed to assess reactivation of MAO-B. In the case of reversible inhibition, the inhibitor will be replaced by the competing excess substrate. The measurements with the reference compound **7** and the inhibitors **8**, **9**, **17**, and **35**, clearly indicated the expected reversible mode of interaction because an elevated fluorescence could be detected after increasing the substrate concentration. In contrast, in the

experiment with the irreversible inhibitor **6**, the residual activity was not enhanced, as expected. These results clearly showed that the benzothiazinones are reversible inhibitors of MAO-B.

To further characterize the interaction of the benzothiazinones with MAO-B, the type of enzyme inhibition was determined by Michaelis-Menten kinetics. Thus, the initial rates of the MAO-B-catalyzed oxidation of the substrate *p*-tyramine, applied at six different concentrations, were measured in the presence of different concentrations of inhibitor **17**. The results are depicted as double reciprocal Lineweaver-Burk plots in Figure 4.

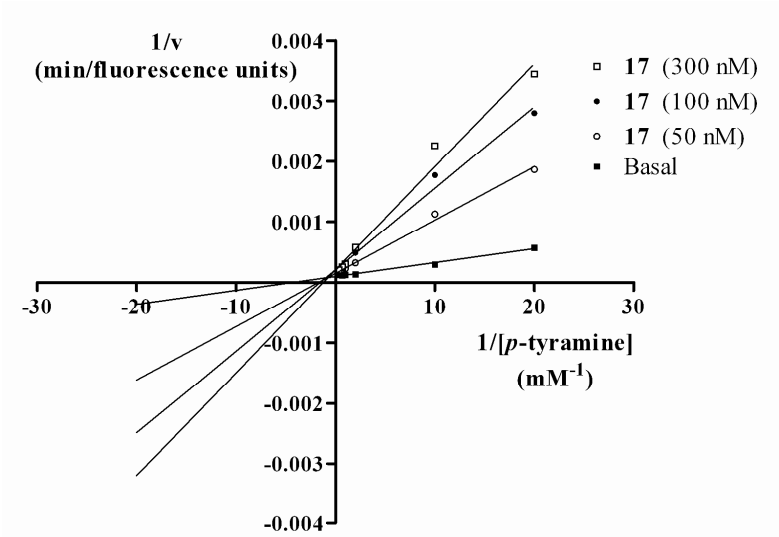

Figure 4. Lineweaver-Burk plot of the inhibition of human MAO-B in the presence of different concentrations of benzothiazinone **17** (0, 50, 100, and 300 nM) with *p*-tyramine (0.05, 0.1, 0.5, 1.0, 1.5, and 3.0 mM) as substrate. The reciprocal MAO-B activity was plotted against the reciprocal substrate concentration (n = 2).

The plots for compound **17** were linear and intersected at the y-axis with the plot for the uninhibited enzyme. These results led us to conclude that the benzothiazinones are competitive inhibitors, which occupy the substrate binding site of MAO-B, in agreement with their reversible mode of interaction.

Identification of Dual-Acting Drugs. With regard to the dual target approach to develop candidates that simultaneously antagonize A_{2A}ARs and inhibit the activity of MAO-B, four derivatives have to be highlighted (**8**, **9**, **17**, and **35**). The corresponding data are summarized in Table 3. We have additionally determined the inhibitory potency of theses compounds towards the human MAO-A. They did not inhibit MAO-A even at high concentrations and could therefore be characterized as selective inhibitors for the isoenzyme MAO-B.

Table 3. Selected Dual-acting 2-Acylaminobenzothiazinones and 2-Acylaminothienothiazinones

		K_i ± SEM (nM)[a]	A_{2A} selectivity			IC_{50} ± SEM (nM)[a]	
compd		**A_{2A}** vs. [^{3}H]MSX-2	hA_1/hA_{2A}	hA_{2B}/hA_{2A}	hA_3/hA_{2A}	**MAO-B**	**MAO-A**
8	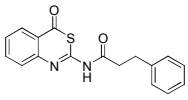	80.9 ± 21.3 (h)[b] 103 ± 10 (r)[c]	13	5	5	17.6 ± 3.7 (h) 42.7 ± 19.8 (r)	>10000 (h)
9	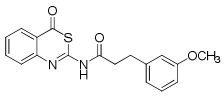	64.9 ± 12.4 (h) 294 ± 137 (r)	21	4	3	95.3 ± 8.8 (h) 621 ± 39 (r)	>10000 (h)
17	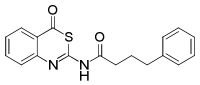	39.5 ± 5.8 (h) 423 ± 76 (r)	63	>25	>25	34.9 ± 2.5 (h) 186 ± 37 (r)	≥10000 (h)
35	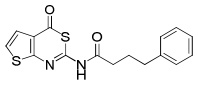	82.5 ± 29.5 (h) 693 ± 141 (r)	4	4	12	69.7 ± 6.1 (h) 291 ± 107 (r)	≥10000 (h)

[a]n = 3. [b](h) Human enzyme. [c](r) Rat enzyme.

The most potent dual-acting compounds **8**, **9**, **17**, and **35** are characterized by a high shape similarity. Considering the benzothiazinone core, an unsubstituted fused benzene ring provided the best activities towards both targets. While the introduction of halogen atoms or methyl groups was not tolerated, the benzene moiety could be replaced by a thiophene isostere retaining the duality of action. An unsubstituted phenylpropionyl or phenylbutyryl moiety turned out to be the most beneficial acyl substituent at the exocyclic 2-amino group. Only for the shorter phenylpropionyl side chain, the attachment of an additional methoxy substituent was allowed without losing dual activity. Compound **17** was the most potent human A_{2A} antagonist (K_i = 39.5 nM) of the whole series and showed high

selectivity over the other adenosine receptor subtypes. Furthermore, **17** had the capability to selectively inhibit human MAO-B in the same nanomolar range (IC_{50} = 34.9 nM). A reduced spacer length in the phenylpropionyl derivative **8** resulted in a better human MAO-B inhibition, but a slightly reduced human A_{2A} affinity and selectivity.

We investigated the stability of compound **17** dissolved in DMSO by LCMS and ^{1}H NMR spectroscopy and compared it to that of standard compound **2** (for details see Figures S2, S3, S4, S5, and Table S1, Supporting Information). In accordance with previously published observations for styrylxanthine derivatives,[27] compound **2** was unstable when exposed to daylight at room temperature, which was already seen after 24 h of incubation. In contrast, **17** was found to be completely stable even after 7 days of incubation under the same conditions.

Our findings indicate the restricted opportunities for scaffold modifications, when addressing two diverse and unrelated protein targets. In general, the development of a dual-acting compound requires a complex design and optimization process to adjust the ratio of activities at the two diverse targets. However, it may be well worth while developing such dual or multiple target-directed drugs. A multiple ligand might be able to enhance efficacy and improve safety compared to a mixture of two compounds each of which addresses only a single target. There is an increasing interest in modulating multiple targets, especially in complex diseases such as PD.

CONCLUSIONS

In conclusion, we discovered 4*H*-3,1-benzothiazin-4-ones and thienothiazinone analogues as a structurally novel class of non-xanthine and non-adenine related compounds with a dual mode of action, targeting A_{2A}ARs and MAO-B at the same time. Twenty eight new compounds were synthesized and investigated in radioligand binding studies at all four adenosine receptor subtypes and in enzyme inhibition studies at MAO-B and MAO-A. Structural optimization and SAR analyses led to the development of potent and selective A_{2A}AR antagonists and the discovery of the first MAO-B inhibitors within the class of benzothiazinones. We were able to identify several ligands potently addressing both targets at similar concentrations. Species differences were determined between the human and the rat ARs. All derivatives showed a preference for the human over the rat A_{2A}AR, while the opposite trend was observed for the A_1AR. A similar observation was made for MAO-B, where in most cases a strong preference for the human enzyme was found. 4*H*-3,1-Benzothiazin-4-one **17** was characterized as a potent and selective A_{2A}AR antagonist and a reversible, competitive MAO-B inhibitor. This compound is a promising new lead structure for dual-acting drugs and may serve as a pharmacological tool for proof-of-concept in vivo studies to validate this dual target approach as a novel strategy for the treatment of PD.

EXPERIMENTAL SECTION

Chemistry. All reagents were obtained from various producers (Acros, Sigma Aldrich, Alfa Aesar, and Fluorochem) and used without further purification. Solvents were used without additional purification or drying unless otherwise noted. Reactions were monitored by thin layer chromatography (TLC) using aluminum sheets coated with silica gel 60 F_{254} (Merck). Compounds were visualized under UV light (254 nm). Preparative column chromatography was performed on silica gel 60 (Acros Organics) 0.060–0.200 mm. Mass spectra were recorded on an API 2000 mass spectrometer (electron spray ion source, Applied Biosystems, Darmstadt, Germany) coupled with an Agilent 1100 HPLC system using a Phenomenex Luna HPLC C18 column (50 × 2.00 mm, particle size 3 µm). The purity of the tested compounds was determined by HPLC-UV obtained on an LC-MS instrument (Applied Biosystems API 2000 LC-MS/MS, HPLC Agilent 1100) using the procedure as follows: dissolving of the compounds at a concentration of 1.0 mg/mL in methanol and if necessary sonicated to complete dissolving. Then, 10 µL of the substance solution was injected into a Phenomenex Luna C18 HPLC column (50 × 2.00 mm, particle size 3 µm) and elution performed with a gradient of water/methanol either containing 2 mM ammonium acetate and 0.1% formic acid (chrom. system A) or 2 mM ammonium acetate (chrom. system B) from 90:10 up to 0:100 for 30 min at a flow rate of 250 µL/min, starting the gradient after 10 min. UV absorption was detected from 220 to 400 nm using a diode array detector. All tested compounds possessed a purity of not less than 95%. ^{1}H and ^{13}C NMR spectra were recorded on a Bruker Avance 500 MHz NMR spectrometer. DMSO-d_6, $CDCl_3$, acetone-d_6 was used as solvents as indicated below. NMR spectra were recorded at room temperature. Chemical shifts are given in parts per million (ppm) relative to the remaining protons of the deuterated solvent used as internal standard. Coupling constants *J* are given in Hertz, and spin multiplicities are given as s (singlet), d (doublet), t (triplet), q (quartet), m (multiplet), br (broad).

Melting points were determined on a Büchi B-545 melting point apparatus and were uncorrected. The benzothiazinones **25** and **44**,[13] **39** and **48** (R' = CH_3, R'' = H and R' = Cl, R'' = H),[28] and the thienothiazinones **49**[28] were prepared as described.

(2-Carboxyethyl)triphenylphosphonium Bromide. 3-Bromopropanoic acid **42** (25.4 g, 165.5 mmol) and triphenylphosphine (45.7 g, 174 mmol) were suspended in acetonitrile (125 mL) and refluxed for 5 h. After stirring for additional 12 h at room temperature, diethylether (200 mL) was added and the mixture was kept at -18 °C for 2 h. The formed precipitate was collected by suction filtration, washed with diethylether and dried in vacuo to obtain the product (54.1 g, 79%) as a colorless powder. The crude product was used in the next step without further purification.

*General Procedure for the Synthesis of Phenylbutenoic Acids **40**.*

(2-Carboxyethyl)triphenylphosphonium bromide (1.2 equiv) was suspended in CH_2Cl_2 (1 mL/mmol) cooled to 0 °C and the appropriate aldehyde **43** (1.0 equiv) was added. After addition of *tert*-BuOK (2.5 equiv) in portions, the reaction mixture was stirred for 12 h at room temperature. The reaction was quenched with water (2 mL/mmol), washed two times with CH_2Cl_2 and adjusted to pH 1. After extraction with diethylether the combined organic layers were washed with brine, dried ($MgSO_4$) and the solvent was rotary evaporated. The crude material was purified by silica gel chromatography as indicated below.

*(E)-4-Phenylbut-3-enoic Acid. **(40, R''' = H)**.* Purification by silica gel chromatography (CH_2Cl_2/MeOH, 15:1 v/v) to obtain a colorless solid (790 mg, 53%); ^{1}H NMR (500 MHz, DMSO-d_6) δ = 3.18 (dd, J = 1.5, 7.1 Hz, 2H), 6.32 (dt, J = 7.1, 15.9 Hz, 1H), 6.48 (d, J = 16.0 Hz, 1H), 7.20 – 7.24 (m, 1H), 7.28 – 7.33 (m, 2H), 7.42 – 7.38 (m, 2H), 12.35 (br, 1H); ^{13}C NMR (125 MHz, DMSO-d_6) δ = 38.0, 123.3, 126.1 (2C), 127.5, 128.7 (2C), 132.4, 136.9, 172.7.

*(E)-4-(3-Methoxyphenyl)but-3-enoic Acid **(40, R''' = 3-OMe)**.* Purification by silica gel chromatography (CH_2Cl_2/MeOH, 10:1 v/v) to obtain a colorless solid (2.12 g, 75%); ^{1}H NMR (500 MHz, DMSO-d_6) δ = 3.17 (dd, J = 1.3, 7.1 Hz, 2H), 3.75 (s, 3H), 6.31 (dt, J = 7.1, 15.9 Hz, 1H), 6.45 (d, J = 16.0 Hz, 1H), 6.80 (dd, J = 2.6, 8.2 Hz, 1H), 6.94 – 6.96 (m, 1H), 7.22 (t, J = 7.9 Hz, 1H), 6.97 (d, J = 7.7 Hz, 1H), 12.32 (br, 1H); ^{13}C NMR (125 MHz, DMSO-d_6) δ = 38.0, 55.2, 111.3, 113.4, 118.7, 123.7, 129.8, 132.4, 138.4, 159.7, 172.7.

*(E)-4-(3-Chlorophenyl)but-3-enoic Acid (**40, R''' = 3-Cl**).* Purification by silica gel chromatography (CH_2Cl_2/MeOH, 15:1 v/v) to obtain a colorless solid (12.6 g, 41%); ^{1}H NMR (500 MHz, DMSO-d_6) δ = 3.19 (dd, *J* = 1.2, 6.9 Hz, 2H), 6.38 (dt, *J* = 6.9, 16.0 Hz, 1H), 6.48 (d, *J* = 16.0 Hz, 1H), 7.27 (ddd, *J* = 1.4, 2.0, 7.7 Hz, 1H), 7.33 (t, *J* = 7.7 Hz, 1H), 7.37 (dt, *J* = 1.4, 7.7 Hz, 1H), 7.46 (t, *J* = 1.8 Hz, 1H), 12.45 (br, 1H); ^{13}C NMR (125 MHz, DMSO-d_6) δ = 38.0, 124.8, 125.4, 125.9, 127.2, 130.6, 131.0, 133.6, 139.2, 172.5.

*(E)-4-(3,4-Dichlorophenyl)but-3-enoic Acid (**40, R''' = 3,4-Cl**).* Purification by silica gel chromatography (CH_2Cl_2/MeOH, 10:1 v/v) to obtain a colorless solid (1.61 g, 61%); ^{1}H NMR (500 MHz, DMSO-d_6) δ = 3.18 (d, *J* = 6.0 Hz, 2H), 6.42 (dt, *J* = 6.3, 16.0 Hz, 1H), 6.47 (d, *J* = 16.1 Hz, 1H), 7.41 (dd, *J* = 2.1, 8.4 Hz, 1H), 7.54 (d, *J* = 8.4 Hz, 1H), 7.66 (d, *J* = 2.0 Hz, 1H), 12.28 (br, 1H); ^{13}C NMR (125 MHz, DMSO-d_6) δ = 38.0, 123.0, 126.2, 126.3, 128.0, 129.7, 130.8, 131.6, 137.8, 172.4.

*General Procedure for the Synthesis of Phenylbutyric Acids **41**.* 10% Pd/C (10 wt%) was added to a solution of the corresponding olefins (**40** or commercially available reagent) in EtOH or THF (3 mL/mmol) and stirred under H_2 atmosphere for 1 h. After filtration through a pad of Celite, the filter cake was rinsed with EtOH or THF and the solvent of the filtrate was removed to obtain the desired product. In some cases purification by silica gel chromatography was necessary as indicated below.

*4-(3-Methoxyphenyl)butanoic Acid (**41, R''' = 3-OMe**).* Light beige solid (587 mg, 97%); ^{1}H NMR (500 MHz, DMSO-d_6) δ = 1.83 – 1.73 (m, 2H), 2.19 (t, *J* = 7.4 Hz, 2H), 2.55 (t, *J* = 7.5 Hz, 2H), 3.72 (s, 3H), 6.71 – 6.78 (m, 3H), 7.01 – 7.27 (m, 1H), 12.13 (br, 1H); ^{13}C NMR (125 MHz, DMSO-d_6) δ = 26.3, 33.2, 34.6, 55.0, 111.4, 114.1, 120.7, 129.4, 143.3, 159.5, 174.4.

*4-(3-Chlorophenyl)butanoic Acid (**41, R''' = 3-Cl**).* Purification by silica gel chromatography (CH_2Cl_2/MeOH, 15:1 → 10:1 v/v) to obtain a colorless oil (345 mg, 38%); ^{1}H NMR (500 MHz, $CDCl_3$) δ = 1.94 (m, 2H), 2.36 (t, *J* = 7.4 Hz, 2H), 2.64 (t, *J* = 7.4 Hz, 2H), 7.04 (d, *J* = 7.4 Hz, 1H), 7.14 – 7.19 (m, 3H), 12.10 (br, 1H); ^{13}C NMR (125 MHz, DMSO-d_6) δ = 26.0, 33.6, 33.8, 126.0, 127.2, 128.4, 130.2, 133.0, 144.6, 174.3.

*4-(3,4-Dichlorophenyl)butanoic Acid (**41, R''' = 3,4-Cl**).* Purification by silica gel chromatography (CH_2Cl_2/MeOH, 15:1 → 10:1 v/v) to obtain a colorless oil (513 mg, 57%); ^{1}H NMR (500 MHz, DMSO-d_6) δ = 1.73 – 1.83 (m, 2H), 2.20 (t, *J* = 7.4 Hz, 2H), 2.58 (t, *J* = 7.5 Hz, 2H), 7.19 (dd, *J* = 2.1, 8.2 Hz, 1H), 7.46 (d, *J* = 2.0 Hz, 1H), 7.52 (d, *J* = 8.2 Hz, 1H), 12.10 (br, 1H); ^{13}C NMR (125 MHz, DMSO-d_6) δ = 26.0, 33.1, 33.5, 128.5, 128.9, 130.48, 130.50, 130.9, 143.1, 174.2.

*3-(2-Fluorophenyl)propanoic Acid (**41, R''' = 2-F**).* Colorless solid (506 mg, quantitative); ^{1}H NMR (500 MHz, $CDCl_3$) δ = 2.68 (t, *J* = 7.8 Hz, 2H), 2.97 (t, *J* = 7.7 Hz, 2H), 6.98 – 7.03 (m, 1H), 7.03 – 7.07 (m, 1H), 7.15 – 7.23 (m, 2H), 10.09 (br, 1H); ^{13}C NMR (125 MHz, DMSO-d_6) δ = 24.3, 34.1, 115.4 (d, *J*(C,F) = 21.8 Hz), 124.1. (d, *J*(C,F) = 16.0 Hz), 127.0 (d, *J*(C,F) = 15.5 Hz), 128.2 (d, *J*(C,F) = 8.1 Hz), 130.6 (d, *J*(C,F) = 4.6 Hz), 161.2 (d, *J*(C,F) = 256 Hz), 178.8.

*2-Amino-6-bromo-4H-3,1-benzothiazin-4-one (**48, R' = Br, R'' = H**).* Benzoyl isothiocyanate (2.00 mL, 15.0 mmol) was added dropwise to a solution of methyl 2-amino-5-bromobenzoate (3.00 g, 13.0 mmol) in acetone (10 mL). After stirring for 20 min at room temperature the formed precipitate was filtered by suction filtration and recrystallized from toluene to obtain the thioureide as a light yellow solid (4.48 g, 87%). The intermediate (1.00 g, 2.54 mmol) was treated with 10 drops water and concentrated H_2SO_4 (7 mL) and stirred for 4 h at 100 °C. After cooling to room temperature the reaction mixture was put carefully into ice water and neutralized by addition of solid $NaHCO_3$. The formed precipitate was filtered by suction filtration and dried in vacuo. After recrystallization from toluene the product **48** (R' = Br, R'' = H) was obtained as a light yellow solid (510 mg, 78%); ^{1}H NMR (500 MHz, $CDCl_3$) δ = 7.22 (d, *J* = 8.8 Hz, 1H), 7.77 (dd, *J* = 2.5, 8.8 Hz, 1H), 7.93 (d, *J* = 2.5 Hz, 1H), 8.04 (br, 2H); ^{13}C NMR (125 MHz, DMSO-d_6) δ = 115.0, 117.8, 126.3, 129.9, 138.6, 150.4, 157.5, 183.1; LC/ESI-MS (*m/z*): negative mode 257 $[M-H]^-$, positive mode 259 $[M+H]^+$.

*2-Amino-7-chloro-4H-3,1-benzothiazin-4-one (**48, R' = H, R'' = Cl**).* Benzoyl isothiocyanate (0.90 mL, 6.70 mmol) was added dropwise to a solution of 6-chloroanthranilic acid (1.00 g, 5.80 mmol) in acetone (34 mL). After stirring for 20 min at room temperature the formed precipitate was filtered by suction filtration and recrystallized from MeOH to obtain the thioureide as a light yellow solid (1.55 g, 79%).

The intermediate (1.00 g, 2.99 mmol) was treated with 10 drops water and concentrated H_2SO_4 (20 mL) and stirred for 4 h at 100 °C. After cooling to room temperature the reaction mixture was put carefully into ice water and neutralized by addition of solid $NaHCO_3$. The formed precipitate was filtered by suction filtration and dried in vacuo. After recrystallization from toluene product **48** (R' = H, R'' = Cl) was obtained as a light yellow solid (526 mg, 83%); ^{1}H NMR (500 MHz, $CDCl_3$) δ = 7.19 (dd, *J* = 2.1, 8.6 Hz, 1H), 7.27 (d, *J* = 2.1 Hz, 1H), 7.87 (d, *J* = 8.6 Hz, 1H), 8.09 (br, 2H); ^{13}C NMR (125 MHz, DMSO-d_6) δ = 115.4, 123.4, 126.3, 126.5, 140.7, 152.6, 158.4, 183.2; LC/ESI-MS (*m/z*): negative mode 211 $[M-H]^-$, positive mode 213 $[M+H]^+$.

*General Procedure for Acylation of 2-Amino-4H-3,1-benzothiazin-4-one with the Acids **40** and **41** to Produce 2-Acylamino-4H-3,1-benzothiazin-4-ones (**8-24**).* *N*-Methylmorpholine (1.1 equiv) was added to a solution of the appropriate carboxylic acid **40** or **41** (1.0 equiv) in THF (4 mL/mmol). After the addition of 2,4,6-trichlorobenzoyl chloride (1.1 equiv) the reaction mixture was stirred for 2 h at room temperature. The solvent was removed under reduced pressure and the residue was taken up in toluene (12 mL/mmol). After the addition of pyridine (2.4 equiv) and amine **39** (1 equiv) the mixture was refluxed for 2 h. Then the hot mixture was filtered and the filtrate was cooled. The formed precipitate was collected by suction filtration, washed with petroleum ether and purified as indicated below.

*N-(4-Oxo-4H-3,1-benzothiazin-2-yl)-3-phenylpropanamide (**8**).* Recrystallization two times from toluene afforded **8** as a colorless solid (130 mg, 50%), mp: 186-188 °C (toluene); ^{1}H NMR (500 MHz, DMSO-d_6) δ 2.75 (t, *J* = 7.5 Hz, 2H), 2.88 (t, *J* = 7.7 Hz, 2H), 7.18 (tt, *J* = 1.3, 7.2 Hz, 1H), 7.25 – 7.21 (m, 2H), 7.25 – 7.31 (m, 2H), 7.49 (ddd, *J* = 1.2, 7.3, 8.2 Hz, 1H), 7.57 (dd, *J* = 0.7, 8.2 Hz, 1H), 7.85 (ddd, *J* = 1.6, 7.2, 8.7 Hz, 1H), 8.02 (dd, *J* = 1.4, 8.0 Hz, 1H), 11.89 (br, 1H); ^{13}C NMR (125 MHz, DMSO-d_6) δ 30.1, 37.2, 119.5, 124.4, 126.2, 127.1, 128.4 (2C), 128.5 (2C), 128.9, 136.4, 140.7, 147.7, 153.0, 172.9, 184.5; LC/ESI-MS (*m/z*): negative mode 309 $[M-H]^-$, positive mode 311 $[M+H]^+$; purity: 99% (A), 99% (B).

*3-(3-Methoxyphenyl)-N-(4-oxo-4H-3,1-benzothiazin-2-yl)propanamide (**9**).* Recrystallization two times from toluene afforded **9** as colorless crystals (128 mg, 45%), mp: 168-170 °C (toluene); ^{1}H NMR (500

MHz, DMSO-d_6) δ 2.75 (t, J = 8.1 Hz, 2H), 2.86 (t, J = 7.6 Hz, 2H), 3.72 (s, 3H), 6.75 (ddd, J = 1.2, 2.4, 8.2 Hz, 1H), 6.78 – 6.81 (m, 2H), 7.19 (t, J = 8.0 Hz, 1H), 7.50 (ddd, J = 1.2, 7.4, 15.1 Hz, 1H), 7.57 (ddd, J = 0.5, 1.2, 8.2 Hz, 1H), 7.85 (ddd, J = 1.7, 7.2, 8.2 Hz, 1H), 8.03 (ddd, J = 8.0, 1.6, 0.4 Hz, 1H), 11.89 (br, 1H); ^{13}C NMR (125 MHz, DMSO-d_6) δ 30.2, 37.1, 55.0, 111.6, 114.1, 119.5, 120.6, 124.5, 127.1, 129.0, 136.4, 142.3, 147.7, 153.0, 159.4, 173.0, 177.7, 184.6; LC/ESI-MS (*m/z*): negative mode 339 $[M-H]^-$, positive mode 341 $[M+H]^+$; purity: 95% (A), 95% (B).

*3-(3,4-Dichlorophenyl)-N-(4-oxo-4H-3,1-benzothiazin-2-yl)propanamide (**10**).* Recrystallization from EtOH afforded **10** as a colorless solid (188 mg, 36%), mp: 230 °C (EtOH); ^{1}H NMR (500 MHz, DMSO-d_6) δ 2.77 (t, J = 7.5 Hz, 2H), 2.89 (t, J = 7.5 Hz, 2H), 7.24 (dd, J = 2.0, 8.3 Hz, 1H), 7.48 – 7.56 (m, 3H), 7.57 (dd, J =0.7, 8.2 Hz, 1H), 7.86 (ddd, J = 1.6, 7.2, 8.7 Hz, 1H), 8.03 (dd, J = 1.6, 7.9 Hz, 1H), 11.90 (br, 1H); ^{13}C NMR (125 MHz, DMSO-d_6) δ 29.2, 36.7, 119.5, 124.5, 127.2, 128.8, 128.97, 129.00, 130.6 (2C), 131.0, 136.5, 142.1, 147.7, 153.0, 172.7, 184.5; LC/ESI-MS (*m/z*): negative mode 377 $[M-H]^-$, positive mode 379 $[M+H]^+$; purity: 100% (A), 100% (B).

*3-(2-Fluorophenyl)-N-(4-oxo-4H-3,1-benzothiazin-2-yl)propanamide (**11**).* Recrystallization from EtOH afforded **11** as colorless crystals (140 mg, 48%), mp: 190-192 °C (EtOH); ^{1}H NMR (500 MHz, DMSO-d_6) δ 2.76 (t, J = 7.6 Hz, 2H), 2.91 (t, J = 7.6 Hz, 2H), 7.10 – 7.17 (m, 2H), 7.22 – 7.28 (m, 1H), 7.31 (td, J = 1.5, 7.7 Hz, 1H), 7.50 (ddd, J = 1.2, 7.2, 8.2 Hz, 1H), 7.57 (dd, J = 0.8, 8.2 Hz, 1H), 7.83 – 7.88 (m, 1H), 7.83 (dd, J = 1.4, 8.0 Hz, 1H), 11.91 (br, 1H); ^{13}C NMR (125 MHz, DMSO-d_6) δ 23.4 (d, J (C,F) = 2.5 Hz), 35.7, 115.2 (d, J (C,F) = 21.3 Hz), 119.5, 124.48, 124.55 (d, J (C,F) = 2.5 Hz), 127.2, 127.3 (d, J (C,F) = 16.3 Hz), 128.4 (d, J (C,F) = 7.5 Hz), 129.0, 130.8 (d, J (C,F) = 5.0 Hz), 136.5, 147.7, 153.0, 160.6 (d, J (C,F) = 242 Hz), 172.7, 184.6; LC/ESI-MS (*m/z*): negative mode 327 $[M-H]^-$, positive mode 329 $[M+H]^+$; purity: 96% (A), 100% (B).

*3-(2-Bromophenyl)-N-(4-oxo-4H-3,1-benzothiazin-2-yl)propanamide (**12**).* Recrystallization from EtOH afforded **12** as colorless crystals (253 mg, 52%), mp: 195 °C (EtOH); ^{1}H NMR (500 MHz, DMSO-d_6) δ 2.77 (t, J = 7.7 Hz, 2H), 2.99 (t, J = 7.7 Hz, 2H), 7.16 (ddd, J = 2.0, 7.2, 8.0 Hz, 1H), 7.35 (td, J = 2.0, 7.2, 8.0 Hz, 1H), 7.36 (dd, J = 1.9, 7.7 Hz, 1H), 7.51 (ddd, J = 1.0, 7.0, 8.0 Hz, 1H), 7.51 – 7.56 (m,

2H), 7.86 (ddd, *J* = 1.6, 7.2, 8.2 Hz, 1H), 8.03 (ddd, *J* = 0.4, 1.5, 8.0 Hz, 1H), 11.94 (br, 1H); ^{13}C NMR (125 MHz, DMSO-d_6) δ 30.5, 35.4, 119.5, 123.9, 124.5, 127.2, 128.1, 128.6, 129.0, 130.7, 132.7, 136.5, 139.7, 147.7, 153.0, 172.5, 184.6; LC/ESI-MS (*m/z*): negative mode 387 $[M-H]^-$, positive mode 389 $[M+H]^+$; purity: 100% (A), 100% (B).

*2-(3-Chlorophenoxy)-N-(4-oxo-4H-3,1-benzothiazin-2-yl)acetamide (**13**).* Recrystallization from EtOH afforded **13** as a colorless solid (142 mg, 57%), mp: 188-189 °C (EtOH); ^{1}H NMR (500 MHz, DMSO-d_6) δ 4.99 (s, 2H), 6.98 (td, *J* = 1.3, 7.7 Hz, 1H), 7.06 (dd, *J* = 1.2, 8.3 Hz, 1H), 7.28 (ddd, *J* = 1.6, 7.5, 8.4 Hz, 1H), 7.44 (dd, *J* = 1.6, 7.9 Hz, 1H), 7.53 (td, *J* = 1.1, 8.1 Hz, 1H), 7.62 (dd, *J* = 0.8, 8.2 Hz, 1H), 7.88 (ddd, *J* = 1.6, 7.2, 8.7 Hz, 1H), 8.05 (dd, *J* = 1.4, 8.0 Hz, 1H), 12.09 (br, 1H); ^{13}C NMR (125 MHz, DMSO-d_6) δ 66.8, 114.0, 119.4, 121.5, 122.4, 124.6, 127.5, 128.4, 129.2, 130.3, 136.6, 147.5, 152.4, 153.3, 168.5, 184.1; LC/ESI-MS (*m/z*): negative mode 345 $[M-H]^-$, positive mode 347 $[M+H]^+$; purity: 97% (A), 96% (B).

*(E)-3-(3-Methoxyphenyl)-N-(4-oxo-4H-3,1-benzothiazin-2-yl)acrylamide (**14**).* The crude material was recrystallized from toluene and purified by silica gel chromatography (CH_2Cl_2/MeOH, 50:1 v/v) to obtain **14** as colorless crystals (61.0 mg, 16%), mp: 182-184 °C; ^{1}H NMR (500 MHz, DMSO-d_6) δ 3.79 (s, 3H), 6.96 (d, *J* = 15.8 Hz, 1H), 7.01 (dd, *J* = 2.2, 7.9 Hz, 1H), 7.15 – 7.18 (m, 1H), 7.20 (d, *J* = 7.6 Hz, 1H), 7.36 (t, *J* = 7.9 Hz, 1H), 7.50 (ddd, *J* = 1.2, 7.2, 8.2 Hz, 1H), 7.60 (dd, *J* = 0.8, 8.2 Hz, 1H), 7.68 (d, *J* = 15.8 Hz, 1H), 7.86 (ddd, *J* = 1.5, 7.0, 8.8 Hz, 1H), 8.03 (dd, *J* = 1.5, 8.0 Hz, 1H), 12.02 (br, 1H), ^{13}C NMR (125 MHz, DMSO-d_6) δ 55.3, 113.6, 116.4, 119.5, 120.1, 120.4, 124.5, 127.2, 129.1, 130.3, 135.6, 136.4, 143.5, 147.7, 153.4, 159.7, 165.2, 184.6; LC/ESI-MS (*m/z*): negative mode 337 $[M-H]^-$, positive mode 339 $[M+H]^+$; purity: 97% (A), 98% (B).

*(E)-3-(3-Chlorophenyl)-N-(4-oxo-4H-3,1-benzothiazin-2-yl)acrylamide (**15**).* The crude material was recrystallized from toluene and purified by silica gel chromatography (CH_2Cl_2/MeOH, 100:1 v/v) to obtain **15** as a colorless solid (72 mg, 19%), mp: 246-247 °C; ^{1}H NMR (500 MHz,) δ 7.00 (d, *J* = 15.8 Hz, 1H), 7.47 – 7.56 (m, 3H), 7.58 – 7.61 (m, 1H), 7.63 (dd, *J* = 0.8, 8.2 Hz, 1H), 7.68 – 7.71 (m, 1H), 7.72 (d, *J* = 15.8 Hz, 1H), 7.88 (ddd, *J* = 1.6, 7.2, 8.2 Hz, 1H), 8.06 (dd, *J* = 1.4, 8.0 Hz, 1H), 12.10 (br,

1H), ^{13}C-NMR (125 MHz, DMSO-d_6) δ 119.5, 121.4, 124.5, 126.5, 127.2, 128.0, 129.0, 130.2, 131.0, 134.0, 136.46, 136.50, 141.9, 147.7, 153.3, 164.9, 184.6; LC/ESI-MS (*m/z*): negative mode 341 $[M-H]^-$, positive mode 343 $[M+H]^+$; purity: 97% (A), 95% (B).

*3-(3-Methoxyphenyl)-N-(4-oxo-4H-3,1-benzothiazin-2-yl)propiolamide (**16**).* The crude material was recrystallized from toluene and purified by silica gel chromatography (CH_2Cl_2/MeOH, 100:1 v/v) to obtain **16** as a colorless solid (104 mg, 27%), mp: 172-174 °C; ^{1}H NMR (500 MHz, DMSO-d_6) δ 3.80 (s, 3H), 7.14 (dd, *J* = 2.1, 8.3 Hz, 1H), 7.22 (s, 1H), 7.25 (d, *J* = 7.5 Hz, 1H), 7.41 (t, *J* = 7.9 Hz, 1H), 7.54 (t, *J* = 7.5 Hz, 1H), 7.63 (d, *J* = 8.1 Hz, 1H), 7.89 (t, *J* = 7.6 Hz, 1H), 8.05 (d, *J* = 7.9 Hz, 1H), 12.76 (br, 1H); ^{13}C NMR (125 MHz, DMSO-d_6) δ 55.5, 82.5, 88.7, 117.4, 118.0, 119.4, 120.1, 124.6, 125.2, 127.6, 129.1, 130.4, 136.6, 147.2, 152.2, 152.8, 159.3, 184.0; LC/ESI-MS (*m/z*): negative mode 335 $[M-H]^-$, positive mode 337 $[M+H]^+$; purity: 95% (A), 95% (B).

*N-(4-Oxo-4H-3,1-benzothiazin-2-yl)-4-phenylbutanamide (**17**).* Recrystallization from EtOH afforded **17** as colorless crystals (340 mg, 47%), mp: 185 °C (EtOH); ^{1}H NMR (500 MHz, DMSO-d_6) δ = 1.83 – 1.90 (m, 2H), 2.46 (t, *J* = 7.4 Hz, 2H), 2.60 (t, *J* = 7.7 Hz, 2H), 7.14 – 7.21 (m, 3H), 7.25 – 7.29 (m, 2H), 7.49 (ddd, *J* = 1.3, 7.3, 8.0 Hz, 1H), 7.57 (dd, *J* = 0.6, 8.2 Hz, 1H), 7.85 (ddd, *J* = 1.6, 7.3, 8.2 Hz, 1H), 8.02 (dd, *J* = 1.3, 8.2 Hz, 1H), 11.84 (br, 1H); ^{13}C NMR (125 MHz, DMSO-d_6) δ = 26.1, 34.5, 35.0, 119.5, 124.4, 126.0, 127.1, 128.4 (2C), 128.5 (2C), 129.0, 136.4, 141.5, 147.8, 153.1, 173.6, 184.7; LC/ESI-MS (*m/z*): negative mode 323 $[M-H]^-$, positive mode 325 $[M+H]^+$; purity: 97% (A), 99% (B).

*4-(3-Methoxyphenyl)-N-(4-oxo-4H-3,1-benzothiazin-2-yl)butanamide (**18**).* Recrystallization two times from EtOH afforded **18** as colorless crystals (604 mg, 65%), mp: 130-132 °C (EtOH); ^{1}H NMR (500 MHz, DMSO-d_6) δ = 1.86 (q, *J* = 7.0 Hz, 2H), 2.45 (t, *J* = 7.4 Hz, 2H), 2.57 (t, *J* = 7.5 Hz, 2H), 3.72 (s, 3H), 6.71 – 6.79 (m, 3H), 7.18 (t, *J* = 8.0 Hz, 1H), 7.49 (ddd, *J* = 1.2, 7.2, 8.2 Hz, 1H), 7.57 (dd, *J* = 0.8, 8.2 Hz, 1H), 7.85 (ddd, *J* = 1.7, 7.2, 8.3 Hz, 1H), 8.02 (dd, *J* = 1.4, 8.2 Hz, 1H), 11.84 (br, 1H); ^{13}C NMR (125 MHz, DMSO-d_6) δ = 25.9, 34.6, 35.0, 55.0, 111.5, 114.1, 119.5, 120.7, 124.5, 127.1, 129.0,

129.4, 136.4, 143.1, 147.8, 153.1, 159.4, 173.6, 184.7; LC/ESI-MS (*m/z*): negative mode 353 $[M-H]^-$, positive mode 355 $[M+H]^+$; purity: 99% (A), 100% (B).

*4-(3-Chlorophenyl)-N-(4-oxo-4H-3,1-benzothiazin-2-yl)butanamide (**19**).* Recrystallization from EtOH afforded **19** as colorless crystals (112 mg, 37%), mp: 177 °C (EtOH); ^{1}H NMR (500 MHz, DMSO-d_6) δ 1.87 (q, J = 7.5 Hz, 2H), 2.45 (t, J = 7.4 Hz, 2H), 2.62 (t, J = 7.5 Hz, 2H), 7.15 – 7.25 (m, 2H), 7.25 – 7.33 (m, 2H), 7.50 (ddd, J = 1.0, 7.0, 8.0 Hz, 1H), 7.57 (dd, J = 0.7, 8.2 Hz, 1H), 7.86 (ddd, J = 1.6, 7.2, 8.7 Hz, 1H), 8.03 (dd, J = 1.4, 8.0 Hz, 1H), 11.84 (br, 1H); ^{13}C NMR (125 MHz, DMSO-d_6) δ 25.7, 34.1, 34.9, 119.5, 124.5, 126.0, 127.1, 127.3, 128.4, 129.0, 130.3, 133.1, 136.4, 144.2, 148.0, 153.1, 173.5, 184.7; LC/ESI-MS (*m/z*): negative mode 359 $[M-H]^-$, positive mode 357 $[M+H]^+$; purity: 96% (A), 96% (B).

*4-(3,4-Dichlorophenyl)-N-(4-oxo-4H-3,1-benzothiazin-2-yl)butanamide (**20**).* Recrystallization from EtOH afforded **20** as a light beige solid (233 mg, 41%), mp: 200-201 °C (EtOH); ^{1}H NMR (500 MHz, DMSO-d_6) δ 1.87 (q, J = 7.5 Hz, 2H), 2.44 (t, J = 7.3 Hz, 2H), 2.62 (t, J = 7.5 Hz, 2H), 7.21 (dd, J = 2.0, 8.2 Hz, 1H), 7.46 – 7.54 (m, 3H), 7.57 (dd, J = 0.6, 8.2 Hz, 1H), 7.86 (ddd, J = 1.6, 7.2, 8.7 Hz, 1H), 8.03 (dd, J = 1.3, 8.0 Hz, 1H), 11.82 (br, 1H); ^{13}C NMR (125 MHz, DMSO-d_6) δ 25.5, 33.4, 34.8, 119.5, 124.4, 127.1, 128.6, 128.97, 129.03, 130.5, 130.6, 130.9, 136.4, 142.8, 147.8, 153.0, 173.4, 184.6; LC/ESI-MS (*m/z*): negative mode $[M-H]^-$, 391 positive mode 393 $[M+H]^+$; purity: 100% (A), 98% (B).

*(E)-N-(4-Oxo-4H-3,1-benzothiazin-2-yl)-4-phenylbut-3-enamide (**21**).* Recrystallization from EtOH afforded **21** as colorless crystals (91.0 mg, 30%), mp: 180-181 °C (EtOH); ^{1}H NMR (500 MHz, DMSO-d_6) δ 3.41 (dd, J = 1.2, 7.1 Hz, 2H), 6.35 (dt, J = 7.1, 16.0 Hz, 1H), 6.55 (d, J = 16.0 Hz, 1H), 7.23 (dd, J = 4.2, 10.4 Hz, 1H), 7.32 (dd, J = 4.8, 10.4 Hz, 1H), 7.39 – 7.44 (m, 2H), 7.48 – 7.54 (m, 2H), 7.59 (dd, J = 0.7, 8.2 Hz, 1H), 7.84 – 7.89 (m, 1H), 8.03 (dd, J = 1.4, 8.0 Hz, 1H), 11.98 (br, 1H); ^{13}C NMR (125 MHz, DMSO-d_6) δ 25.7, 34.1, 34.9, 119.5, 124.5, 126.0, 127.1, 127.3, 128.4, 129.0, 130.3, 133.1, 136.4, 144.2, 184.7, 147.8, 153.1, 173.5; LC/ESI-MS (*m/z*): positive mode 323 $[M+H]^+$; purity: 98% (A), 97% (B).

*(E)-4-(3-Methoxyphenyl)-N-(4-oxo-4H-3,1-benzothiazin-2-yl)but-3-enamide (**22**).* The crude material was recrystallized from toluene and purified by silica gel chromatography using CH_2Cl_2 as eluent to obtain **22** as colorless crystals (126 mg, 28%), mp: 167 °C; ^{1}H NMR (500 MHz, DMSO-d_6) δ 3.40 (dd, J = 1.3, 7.0 Hz, 2H), 3.75 (s, 3H), 6.36 (dt, J = 7.0, 15.9 Hz, 1H), 6.52 (d, J = 15.9 Hz, 1H), 6.80 (ddd, J = 0.8, 2.5, 8.2 Hz, 1H), 6.95 – 7.02 (m, 2H), 7.23 (t, J = 7.9 Hz, 1H), 7.50 (ddd, J = 1.0, 7.0, 8.0 Hz, 1H), 7.59 (dd, J =0.8, 8.2 Hz, 1H), 7.86 (ddd, J = 1.6, 7.2, 8.2 Hz, 1H), 8.03 (dd, J = 1.3, 8.0 Hz, 1H), 11.97 (br, 1H); ^{13}C NMR (125 MHz, DMSO-d_6) δ 40.0, 55.2, 111.4, 113.5, 118.8, 119.5, 122.8, 124.5, 127.2, 129.0, 129.8, 133.3, 136.5, 138.2, 147.7, 153.1, 159.7, 171.6, 184.5; LC/ESI-MS (*m/z*): negative mode 351 $[M-H]^-$, positive mode 353 $[M+H]^+$; purity: 96% (A),97% (B).

*(E)-4-(3-Chlorophenyl)-N-(4-oxo-4H-3,1-benzothiazin-2-yl)but-3-enamide (**23**).* The crude material was purified by silica gel chromatography (petroleum ether/ethyl acetate, 1:1 v/v) and recrystallized from EtOH to obtain **23** as a colorless solid (178 mg, 20%), mp: 197 °C (EtOH); ^{1}H NMR (500 MHz, DMSO-d_6) δ = 3.42 (dd, J = 1.1, 6.9 Hz, 2H), 6.45 (dt, J = 6.9, 16.0 Hz, 1H), 6.55 (d, J = 16.0 Hz, 1H), 7.29 (ddd, J = 1.2, 2.1, 7.9 Hz, 1H), 7.35 (t, J = 7.8 Hz, 1H), 7.40 (dt, J = 1.3, 7.7 Hz, 1H), 7.46 – 7.54 (m, 2H), 7.61 (dd, J = 0.8, 8.2 Hz, 1H), 7.88 (ddd, J = 1.7, 7.2, 8.2 Hz, 1H), 8.04 (dd, J = 1.3, 8.0 Hz, 1H), 12.00 (br, 1H); ^{13}C NMR (125 MHz, DMSO-d_6) δ = 39.6, 119.5, 124.50, 124.54, 124.9 125.9, 127.3, 127.4, 129.1, 130.6, 131.9, 133.6, 136.5, 139.0, 147.7, 153.0, 171.4, 184.5; LC/ESI-MS (*m/z*): negative mode 355 $[M-H]^-$, positive mode 357 $[M+H]^+$; purity: 99% (A), 99% (B).

*(E)-4-(3,4-Dichlorophenyl)-N-(4-oxo-4H-3,1-benzothiazin-2-yl)but-3-enamide (**24**).* The crude material was purified by silica gel chromatography using CH_2Cl_2 as eluent and recrystallized from toluene to obtain **24** as a light beige solid (116 mg, 18%), mp: 215 °C (toluene); ^{1}H NMR (500 MHz, aceton-d_6) δ 3.57 (d, J = 6.1 Hz, 2H), 6.57 (dt, J = 6.6, 16.0 Hz, 1H), 6.64 (d, J = 16.0 Hz, 1H), 7.44 – 7.56 (m, 4H), 7.66 (d, J = 2.0 Hz, 1H), 7.82 (ddd, J = 1.6, 7.2, 8.3 Hz, 1H), 8.08 (dd, J = 8.0, 1.6 Hz, 1H), 10.71 (br, 1H); ^{13}C NMR (125 MHz, DMSO-d_6) δ 40.0, 119.5, 124.5, 125.4, 126.3, 127.3, 128.1, 129.1, 129.8, 130.85, 130.88, 131.6, 136.5, 137.6, 147.7, 153.0, 171.3, 184.5; LC/ESI-MS (*m/z*): positive mode 391 $[M+H]^+$; purity: 98% (A), 97% (B).

*General Procedure for the Amide Coupling of Compound **44** with the Piperazines **45** (**26-28**).* 1,1'-Carbonyldiimidazole (1.1 equiv) was added to 4-(4-oxo-4*H*-3,1-benzothiazin-2-ylcarbamoyl)benzoic acid **44** (1 equiv) dissolved in DMF (6 mL/mmol) and stirred at room temperature for 1 h. To a solution of the piperazine derivative **45** (1.25 equiv) in DMF/1,4-dioxane (1:1, 2 mL/mmol) imidazole (1.0 equiv) and HCl (2.0 equiv, 4 N in 1,4-dioxane) were added dropwise. The two mixtures were combined, stirred at room temperature for 2 h and poured into saturated aqueous $NaHCO_3$ solution (~100 mL/mmol). The precipitate was collected by suction filtration, dried and recrystallized from EtOH.

4-(4-(2-Chlorobenzyl)piperazine-1-carbonyl)-N-(4-oxo-4H-3,1-benzothiazin-2-yl)benzamide ***(26)***. Colorless solid (109 mg, 23%), mp: 230-232 °C (EtOH); ^{1}H NMR (500 MHz, DMSO-d_6) δ 2.42 (br, 2H), 3.29 (br, 4H), 3.61 (s, 2H), 3.67 (br, 2H), 7.28 (td, J = 1.9, 7.6 Hz, 1H), 7.32 (td, J = 1.5, 7.4 Hz, 1H), 7.39 – 7.46 (m, 2H), 7.46 – 7.52 (m, 3H), 7.57 – 7.63 (m, 1H), 7.77 – 7.85 (m, 1H), 7.99 – 8.04 (m, 1H), 8.09 – 8.13 (m, 2H), 12.41 (br, 1H); ^{13}C NMR (125 MHz, DMSO-d_6) δ 41.8, 47.3, 52.4, 53.0, 58.6, 119.5, 124.4, 126.2, 126.9, 127.2, 128.5, 128.9 (2C), 129.4, 131.1, 133.5, 135.4, 136.1, 139.5, 148.3, 168.3, 176.9, 185.9; LC/ESI-MS (*m/z*): negative mode 517 $[M-H]^-$, positive mode 519 $[M+H]^+$; purity: 99% (B).

4-(4-(3-Chlorobenzyl)piperazine-1-carbonyl)-N-(4-oxo-4H-3,1-benzothiazin-2-yl)benzamide ***(27)***. Colorless solid (163 mg, 34%), mp: 243-244 °C (EtOH); ^{1}H NMR (500 MHz, DMSO-d_6) δ 2.36 (br, 2H), 2.43 (br, 2H), 3.29 (br, 2H), 3.52 (s, 2H), 3.65 (br, 2H), 7.25 – 7.29 (m, 1H), 7.29 – 7.32 (m, 1H), 7.34 (d, J = 7.4 Hz, 1H), 7.36 – 7.38 (m, 1H), 7.50 – 7.56 (m, 3H), 7.66 – 7.69 (m, 1H), 7.89 (ddd, J = 1.6, 7.2, 8.3 Hz, 1H), 8.06 (dd, J = 1.5, 8.0 Hz, 1H), 8.08 – 8.12 (m, 2H), 12.39 (br, 1H); ^{13}C NMR (125 MHz, DMSO-d_6) δ 41.7, 47.2, 52.2, 52.7, 61.1, 119.6, 124.6, 127.1, 127.2, 127.6, 128.6, 128.9 (2C), 130.2, 132.5, 133.1, 136.5, 140.2, 140.8, 148.9, 167.5, 168.1, 184.7; LC/ESI-MS (*m/z*): negative mode 517 $[M-H]^-$, positive mode 519 $[M+H]^+$; purity: 100% (B).

4-(4-(4-Chlorobenzyl)piperazine-1-carbonyl)-N-(4-oxo-4H-3,1-benzothiazin-2-yl)benzamide ***(28)***. Colorless solid (83.0 mg, 17%), mp: 240-243 °C (EtOH); ^{1}H NMR (500 MHz, DMSO-d_6) δ 2.35 (br, 2H), 2.43 (br, 2H), 3.29 (br, 2H), 3.50 (s, 2H), 3.63 (br, 2H), 7.31 – 7.35 (m, J = 8.6, 2H), 7.35 – 7.39

(m, 2H), 7.49 – 7.56 (m, 3H), 7.65 – 7.69 (m, 1H), 7.87 – 7.92 (m, 1H), 8.06 (dd, *J* = 1.5, 8.0 Hz, 1H), 8.08 – 8.12 (m, 2H), 12.47 (br, 1H); ^{13}C NMR (125 MHz, DMSO-d_6) δ 41.7, 47.2, 52.2, 52.7, 61.0, 119.5, 124.6, 127.0, 127.2, 128.3 (2C), 128.9, 130.8 (2C), 131.7, 133.2, 136.5, 137.0, 140.2, 147.1, 168.1, 168.3, 184.7; LC/ESI-MS (*m/z*): negative mode 517 $[M-H]^-$, positive mode 519 $[M+H]^+$; purity: 95% (B).

*N-Methyl-N-(4-oxo-4H-3,1-benzothiazin-2-yl)-4-phenylbutanamide (**29**).* Iodomethane (19 µl, 0.31 mmol) was added dropwise to in ice cooled solution of **17** (100 mg, 0.31 mmol) in THF (5 mL). After the addition of sodium hydride (12.0 mg, 0.31 mmol) the reaction mixture was stirred for 24 h at room temperature. The solvent was removed under reduced pressure and the obtained residue was treated with water (5 mL) and extracted with CH_2Cl_2 (3 x 4 mL). The combined organic layers were washed with brine, dried ($MgSO_4$) and the solvents were rotary evaporated. The crude material was absorbed on silica gel and purified by silica gel chromatography (petroleum ether/ethyl acetate, 5:1 v/v) to obtain **29** as a colorless solid (40 mg, 38%), mp: 150 °C; ^{1}H NMR (500 MHz, DMSO-d_6) δ 1.89 (dt, *J* = 7.5, 15.0 Hz, 2H), 2.64 (t, *J* = 7.5 Hz, 2H), 2.74 (t, *J* = 7.3 Hz, 2H), 3.52 (s, 3H), 7.15 – 7.19 (m, 1H), 7.19 – 7.23 (m, 2H), 7.25 – 7.30 (m, 2H), 7.56 (ddd, *J* = 1.2, 7.3, 8.3 Hz, 1H), 7.69 (dd, *J* = 0.9, 8.2 Hz, 1H), 7.90 (ddd, *J* = 1.5, 7.0, 8.0 Hz, 1H), 8.05 (dd, *J* = 1.6, 7.9 Hz, 1H); ^{13}C NMR (125 MHz, DMSO-d_6) δ 25.9, 34.4 (2C), 35.1, 119.1, 124.3, 126.0, 127.8, 128.4 (2C), 128.5 (2C), 129.9, 136.4, 141.7, 146.9, 154.3, 175.3, 185.7; LC/ESI-MS (*m/z*): positive mode 339 $[M+H]^+$; purity: 96% (B).

*General Procedure for Acylation of Compounds **48** and **49** with 4-Phenylbutyric Acid (**30-36**).* *N*-Methylmorpholine (1.1 equiv) was added to a solution of 4-phenylbutyric acid (1.0 equiv) in THF (4 mL/mmol). After the addition of 2,4,6-trichlorobenzoyl chloride (1.1 equiv) the reaction mixture was stirred for 2 h at room temperature. The solvent was removed under reduced pressure and the residue was taken up in toluene (12 mL/mmol). After the addition of pyridine (2.4 equiv) and amine **48** or **49** (1 equiv) the mixture was refluxed for 2 h. Then the hot mixture was filtered and the filtrate was cooled. The formed precipitate was collected by suction filtration, washed with petroleum ether and recrystallized from EtOH.

*N-(6-Methyl-4-oxo-4H-3,1-benzothiazin-2-yl)-4-phenylbutanamide (**30**)*. Colorless crystals (144 mg, 43%), mp: 175-176 °C (EtOH); ^{1}H NMR (500 MHz, DMSO-d_6) δ 1.86 (dt, J = 7.5, 15.0 Hz, 2H), 2.41 (s, 3H), 2.45 (t, J = 7.5 Hz, 2H), 2.60 (t, J = 7.5 Hz, 2H), 7.14 – 7.22 (m, 3H), 7.24 – 7.30 (m, 2H), 7.48 (d, J = 8.3 Hz, 1H), 7.68 (dd, J = 2.0, 8.5 Hz, 1H), 7.83 (d, J = 0.9 Hz, 1H), 11.78 (br, 1H); ^{13}C NMR (125 MHz, DMSO-d_6) δ 20.7, 26.1, 34.5, 35.0, 119.2, 123.9, 126.0, 128.41 (2C), 128.44 (2C), 128.9, 137.0, 141.5, 137.5, 145.7, 152.1, 173.4, 184.6; LC/ESI-MS (*m/z*): negative mode 337 $[M-H]^-$, positive mode 339 $[M+H]^+$; purity: 100% (A), 100% (B).

*N-(6-Chloro-4-oxo-4H-3,1-benzothiazin-2-yl)-4-phenylbutanamide (**31**)*. Colorless crystals (147 mg, 44%), mp: 208-209 °C (EtOH); ^{1}H NMR (500 MHz, DMSO-d_6) δ 1.86 (dt, J = 7.5, 15.0 Hz, 2H), 2.46 (t, J = 7.5 Hz, 2H), 2.59 (t, J = 7.5 Hz, 2H), 7.14 – 7.22 (m, 3H), 7.24 – 7.30 (m, 2H), 7.56 (d, J = 8.8 Hz, 1H), 7.86 (dd, J = 2.6, 8.7 Hz, 1H), 7.93 (d, J = 2.4 Hz, 1H), 11.94 (br, 1H); ^{13}C NMR (125 MHz, DMSO-d_6) δ 26.0, 34.5, 35.1, 120.3, 123.5, 126.0, 128.4 (2C), 128.5 (2C), 131.1, 131.2, 136.1, 141.5, 146.6, 153.7, 173.7, 183.9; LC/ESI-MS (*m/z*): negative mode 357 $[M-H]^-$, positive mode 359 $[M+H]^+$; purity: 99% (A), 99% (B).

*N-(6-Bromo-4-oxo-4H-3,1-benzothiazin-2-yl)-4-phenylbutanamide (**32**)*. Colorless crystals (121 mg, 39%), mp: 219-220 °C (EtOH); ^{1}H NMR (500 MHz, DMSO-d_6) δ 1.86 (dt, J = 7.5, 15.0 Hz, 2H), 2.46 (t, J = 7.4 Hz, 2H), 2.60 (t, J = 7.5 Hz, 2H), 7.14 – 7.22 (m, 3H), 7.24 – 7.30 (m, 2H), 7.50 (d, J = 8.7 Hz, 1H), 7.99 (dd, J = 2.5, 8.7 Hz, 1H), 8.07 (d, J = 2.4 Hz, 1H), 11.95 (br, 1H); ^{13}C NMR (125 MHz, DMSO-d_6) δ 26.0, 34.5, 35.1, 119.3, 120.7, 126.0, 126.5, 128.42 (2C), 128.44 (2C), 131.2, 138.9, 141.5, 146.9, 153.8, 173.7, 183.8; LC/ESI-MS (*m/z*): negative mode 403 $[M-H]^-$, positive mode 405 $[M+H]^+$; purity: 99% (A), 99% (B).

*N-(7-Chloro-4-oxo-4H-3,1-benzothiazin-2-yl)-4-phenylbutanamide (**33**)*. Colorless crystals (163 mg, 48%), mp: 176 °C (EtOH); ^{1}H NMR (500 MHz, DMSO-d_6) δ 1.86 (dt, J = 7.5, 15.0 Hz, 2H), 2.46 (t, J = 7.5 Hz, 2H), 2.59 (t, J = 7.5 Hz, 2H), 7.14 – 7.22 (m, 3H), 7.24 – 7.31 (m, 2H), 7.49 – 7.54 (m, 2H), 8.00 (dd, J = 0.8, 8.1 Hz, 1H), 11.97 (br, 1H); ^{13}C NMR (125 MHz, DMSO-d_6) δ 26.0, 34.5, 35.1,

118.3, 126.0, 126.6, 127.1, 127.9, 128.4 (2C), 128.5 (2C), 140.9, 141.5, 149.1, 155.0, 173.8, 183.9; LC/ESI-MS (*m/z*): negative mode 357 $[M-H]^-$, positive mode 359 $[M+H]^+$; purity: 98% (A), 99% (B).

N-(4-Oxo-4H-thieno[3,2-d][1,3]thiazin-2-yl)-4-phenylbutanamide ***(34)***. Colorless crystals (166 mg, 66%), mp: 194 °C (EtOH); ^{1}H NMR (500 MHz, DMSO-d_6) δ 1.87 (dt, J = 7.5, 14.9 Hz, 2H), 2.47 (t, J = 7.5 Hz, 2H), 2.60 (t, J = 7.5 Hz, 2H), 7.13 – 7.21 (m, 3H), 7.23 – 7.30 (m, 2H), 7.36 (d, J = 5.3 Hz, 1H), 8.34 (d, J = 5.3 Hz, 1H), 12.05 (br, 1H); ^{13}C NMR (125 MHz, DMSO-d_6) δ 26.0, 34.5, 35.0, 118.4, 125.9, 127.4, 128.40 (2C), 128.42 (2C), 136.8, 141.5, 156.8, 158.7, 173.3, 176.0; LC/ESI-MS (*m/z*): negative mode 329 $[M-H]^-$, positive mode 331 $[M+H]^+$; purity: 99% (A), 99% (B).

N-(4-Oxo-4H-thieno[2,3-d][1,3]thiazin-2-yl)-4-phenylbutanamide ***(35)***. Light beige crystals (119 mg, 43%), mp: 174-175 °C (EtOH); ^{1}H NMR (500 MHz, DMSO-d_6) δ 1.87 (dt, J = 7.5, 15.0 Hz, 2H), 2.46 (t, J = 7.4 Hz, 2H), 2.60 (t, J = 7.5 Hz, 2H), 7.14 – 7.22 (m, 3H), 7.24 – 7.30 (m, 2H), 7.36 (d, J = 5.9 Hz, 1H), 7.54 (d, J = 5.9 Hz, 1H), 12.09 (br, 1H); ^{13}C NMR (125 MHz, DMSO-d_6) δ 26.0, 34.5, 35.1, 119.9, 121.0, 122.7, 126.0, 128.4 (2C), 128.5 (2C), 141.5, 157.9, 165.6, 173.2, 176.9; LC/ESI-MS (*m/z*): negative mode 329 $[M-H]^-$, positive mode 331 $[M+H]^+$; purity: 99% (A), 99% (B).

N-(5,6-Dimethyl-4-oxo-4H-thieno[2,3-d][1,3]thiazin-2-yl)-4-phenylbutanamide ***(36)***. Light beige powder (109 mg, 39%), mp: 235-237 °C (EtOH); ^{1}H NMR (500 MHz, DMSO-d_6) δ 1.85 (dt, J = 7.5, 15.0 Hz, 2H), 2.31 (d, J = 0.7 Hz, 3H), 2.32 (d, J = 0.7 Hz, 3H), 2.43 (t, J = 7.4 Hz, 2H), 2.59 (t, J = 7.4 Hz, 2H), 7.10 – 7.21 (m, 3H), 7.23 – 7.32 (m, 2H), 11.98 (br, 1H); ^{13}C NMR (125 MHz, DMSO-d_6) δ 12.4, 13.7, 26.0, 34.5, 35.0, 119.1, 126.0, 128.2, 128.42 (2C), 128.44 (2C), 128.7, 141.5, 157.0, 163.3, 173.3, 177.3; LC/ESI-MS (*m/z*): negative mode 357 $[M-H]^-$, positive mode 359 $[M+H]^+$; purity: 98% (A), 100% (B).

Biological Experiments. Stock solutions of the compounds were prepared in DMSO; the final concentration of DMSO was 2.5% for radioligand binding assays, 2.4% for cAMP assays, and 1% for the MAO assays. At least three independent experiments were performed, each in duplicate or triplicate.

Radioligand Binding Assays. Radioligands were obtained from the following sources: [^{3}H]CCPA from GE Healthcare (58 Ci/mmol), [^{3}H]MSX-2 from Quotient Bioresearch (84 Ci/mmol), [^{3}H]PSB-603 from

GE Healthcare (73 Ci/mmol) and [^{3}H]PSB-11 (53 Ci/mmol) from Quotient Bioresearch. The nonradioactive precursors of [^{3}H]MSX-2,[39] [^{3}H]PSB-603[40] and [^{3}H]PSB-11[41] were synthesized in our laboratory. Membranes from Chinese hamster ovary (CHO) cells stably transfected with the human A_1, human A_{2A}, human A_{2B}, and human A_3 AR were prepared as described.[40,41,42] Frozen rat brains obtained from Pel Freez, Rogers, Arkansas, USA, were dissected to obtain cortical membrane preparations for A_1 assays, and striatal membrane preparations for A_{2A} assays as described.[39,43] The radioligand concentrations were: [^{3}H]CCPA[43] 1.0 nM (rat and human A_1); [^{3}H]MSX-2[39] 1.0 nM (rat and human A_{2A}); [^{3}H]PSB-603[40] 0.3 nM (human A_{2B}); [^{3}H]PSB-11[41] 1.0 nM (human A_3). Binding assays were performed as described.[44,45,39,41,43] About 30-70 μg/mL of protein were used in the assays. Data were analyzed using GRAPH PAD PRISM Version 4 (San Diego, CA, USA). For the calculation of K_i values by nonlinear regression analysis, the Cheng-Prusoff equation and K_D values of 0.2 nM (rat A_1), 0.61 nM (human A_1) for [^{3}H]CCPA, 8 nM for [^{3}H]MSX-2 (rat A_{2A}) and 7.3 nM (human A_{2A}), 0.41 nM for [^{3}H]PSB-603 (human A_{2B}) and 4.9 nM for [^{3}H]PSB-11 (human A_3) were used.

cAMP Accumulation Assays. Stably transfected CHO cells expressing human A_{2A}ARs were transferred into 24-well plates at a density of 200000 cells/well. After 24 h, the medium was removed and the cells were washed with 1 mL of 37 °C warm Hank's Balanced Salt Solution {HBSS [20 mM HEPES, 13 mM NaCl, 5.5 mM glucose, 5.4 mM KCl, 4.2 mM $NaHCO_3$, 1.25 mM $CaCl_2$, 1 mM $MgCl_2$, 0.8 mM $MgSO_4$, 0.44 mM KH_2PO_4, and 0.34 mM Na_2HPO_4 (pH adjusted to 7.3)]}. Then the cells were incubated in 300 μL of HBSS with adenosine deaminase (ADA, Sigma, 1 unit/mL) at 37 °C and 5% CO_2 for 2 h. Then, 100 μL of the phosphodiesterase inhibitor Ro20−1724 (Hoffmann La Roche; final concentration of 40 μM) was added to each well, and the cells were incubated for 10 min at 37 °C. Subsequently, 50 μL of antagonist solution, and after another 10 min of preincubation, 50 μL of agonist dissolved in HBSS-buffer containing 10% DMSO were added. For assays with NECA in the absence of test compound 50 μL of NECA solution and 50 μL of 10%DMSO/90% HBSS-buffer were added. The cells were stimulated with NECA for 15 min at 37 °C. After incubation the supernatant was removed and 500 μL of 90 °C hot lysis buffer consisting of 4 mM EDTA and 0.01% Triton X-100 (pH adjusted

to 7.3) was added. To quantify the cAMP concentration, competition experiments were performed[46] in a final volume of 120 µL containing 50 µL of cell lysate, 30 µL of a [^{3}H]cAMP solution in lysis buffer (final concentration of 3 nM), and 40 µL of cAMP binding protein diluted in the same buffer (50 µg of protein/vial). For determining cAMP concentrations, 50 µL of various cAMP dilutions were added instead of cell lysate to obtain a standard curve. Total binding was determined in the absence of cAMP, and nonspecific binding to the filters was determined without addition of binding protein. The mixture was incubated for 60 min on ice and filtered through GF/B glass fiber filters using a cell harvester (Brandel). The filters were washed three times with 2-3 mL of ice-cold 50 mM Tris-HCl buffer (pH 7.4) and subsequently transferred into scintillation vials. The liquid scintillation counting of the filters started after incubation for 9 h in 2.5 mL of scintillation cocktail (Lumac). Three separate experiments were performed. The amount of cAMP was determined by comparison to a standard curve generated for each experiment.

Monoamine Oxidase Assays. To obtain the rat MAO-B enzyme, mitochondrial-enriched fractions were isolated from male SD rat livers and stored in sodium phosphate buffer (50 mM, pH 7.4) at -80 °C until used. The recombinant human MAO-B and MAO-A enzymes were expressed in baculovirus-infected insect cells purchased from Sigma Aldrich (M7441, M7316). The assays were carried out at rt in 96-well plates in a final volume of 200 µL. The rat liver mitochondria were pre-treated for 15 min at rt with an aqueous solution (final concentration 30 nM) of clorgyline (Sigma Aldrich M3778) to irreversibly inhibit MAO-A activity. A volume of 2 µL of test compound dissolved in DMSO was added to 90 µL of enzyme solution in sodium phosphate buffer (50 mM, pH 7.4) and incubated for 30 min at rt. In each assay, 12 µg of rat liver mitochondria, or 0.9 µg of recombinant human MAO-B, respectively, were used. The reaction had to be kept protected from light and was started by adding 90 µL of freshly prepared Amplex Red reagent (Invitrogen A12214). The reagent was prepared following the manufacturer's recommendation. For each plate, 1 mg of Amplex Red, dissolved in 200 µL of DMSO and 100 µL of reconstituted horseradish peroxidase (HRP 200 U/mL, Sigma Aldrich P6782) were added to 9700 µL of sodium phosphate buffer (250 mM, pH 7.4). To each well, 20 µL of an aqueous solution

(final concentration 300 μM for rat and 150 μM for human enzyme) of *p*-tyramine (Alfa Aesar A12220) were added to start the enzymatic reaction. The production of hydrogen peroxide and consequently of resorufin was quantified in a microplate fluorescence reader (Polarstar BMG Labtech, excitation 544 nm, emission 590 nm) over 45 min. Non-MAO-B enzyme activity was determined in the presence of standard inhibitor **6** (final concentration 1 μM) and subtracted from the total activity measured. Concentration-response curves of **6** served as a positive control. The human MAO-A assays were performed following the protocol for human MAO-B. Non-MAO-A enzyme activity was determined in the presence of clorgyline (final concentration 1 μM) and subtracted from the total activity measured. Concentration-response curves of clorgyline served as a positive control. All data were analyzed using GRAPH PAD PRISM Version 4 (San Diego, CA, USA).

Monoamine Oxidase Reactivation Experiment. The time-dependent activity measurements were performed using human MAO-B under assay conditions. The test compounds **8**, **9**, **17** and **35** as well as **6** and **7** as reference compounds were examined at their corresponding IC_{80} value. The enzyme/inhibitor mixture was not preincubated. The enzyme reaction was started by the addition of 150 μM of *p*-tyramine. After 22 min, the substrate concentration was increased to a final concentration of 1 mM of *p*-tyramine. The reactivation of the enzyme was monitored by fluorescence measurements over a period of 5 h.

Substrate-Dependent Inhibition Kinetics. To evaluate the mode of MAO-B inhibition, sets of Lineweaver–Burk plots were generated. By applying six different concentrations of the substrate *p*-tyramine (0.05, 0.1, 0.5, 1.0, 1.5 and 3.0 mM), the initial catalytic rates of human MAO-B were measured in the absence and in the presence of three different concentrations (50, 100 and 300 nM) of the inhibitor **17**. The assay conditions and measurements were carried out as described above for the IC_{50} determination. Linear regression analysis was performed using GRAPH PAD PRISM Version 4 (San Diego, CA, USA).

ACKNOWLEDGEMENTS

We thank Dr. Jörg Hockemeyer for helpful discussions, Dr. Jürgen Gäb for preparing compound **25**, Norbert Furtmann for some calculations, Angelika Fischer and Anika Püsche for skillful technical assistance in compound testing, Marion Schneider for LC-MS analyses, and Sabine Terhart-Krabbe and Annette Reiner for NMR measurements. This study was supported by the BMBF (German Federal Ministry for Education and Research) within the BioPharma initiative "Neuroallianz".

SUPPORTING INFORMATION. Plots of rat versus human pK_i (A_1 and A_{2A}ARs) and rat versus human pIC_{50} values (MAO-B), HPLC chromatograms and ^{1}H NMR spectra of compounds **2** and **17**. This material is available free of charge via the Internet at http://pubs.acs.org.

ABBREVIATIONS USED

AC, adenylate cyclase; AR, adenosine receptor; cAMP, cyclic adenosine monophosphate; CCPA, [^{3}H]2-chloro-N^6-cyclopentyladenosine; CHO, Chinese hamster ovary; CPA, N^6-cyclopentyladenosine; DA, dopamine; FAD, flavin adenine dinucleotide; h, human; HRP, horseradish peroxidase; MAO, monoamine oxidase; MSX-2, [^{3}H]3-(3-hydroxypropyl)-7-methyl-8-(*m*-methoxystyryl)-1-propargylxanthine; NECA, 5′-*N*-ethylcarboxamidoadenosine; PD, Parkinson's disease; r, rat; ROS, reactive oxygen species; SAR, structure-activity relationship.

*To whom correspondence should be addressed: Christa Müller and Michael Gütschow, PharmaCenter Bonn, Pharmaceutical Institute, Pharmaceutical Chemistry I, An der Immenburg 4, D-53121 Bonn, Germany. Phone: +49-228-73-2301 (CM), +49-228-732317 (MG). Fax: +49-228-73-2567. E-mail: christa.mueller@uni-bonn.de; guetschow@uni-bonn.de

REFERENCES

1 a) Samii, A.; Nutt, J. G.; Ransom, B. R. Parkinson's disease. *The Lancet* **2004**, *363*, 1783–1793. b) Schwarzschild, M. A.; Agnati, L.; Fuxe, K.; Chen, J. F.; Morelli, M. Targeting adenosine A_{2A} receptors in Parkinson's disease. *Trends Neurosci.* **2006**, *29*, 647–654.

2 Allain, H.; Bentué-Ferre, D.; Akwa, Y. Disease-modifying drugs and Parkinson's disease. *Prog. Neurobiol.* **2008**, *84*, 25–39.

3 a) Rezak, M. Current pharmacotherapeutic treatment options in Parkinson's disease. *Dis. Mon.* **2007**, *53*, 214–222. b) Lees, A. Alternatives to levodopa in the initial treatment of early Parkinson's disease. *Drugs Aging* **2005**, *22*, 731–740. c) Dunkel, P.; Chai, C. L.; Sperlágh, B.; Huleatt P. B.; Mátyus, P. Clinical utility of neuroprotective agents in neurodegenerative diseases: current status of drug development for Alzheimer's, Parkinson's and Huntington's diseases, and amyotrophic lateral sclerosis. *Expert Opin. Investig. Drugs* **2012**, *21*, 1267−1308.

4 Armentero, M. T.; Pinna, A.; Ferré, S.; Lanciego, J. L.; Müller, C. E.; R. Franco. Past, present and future of A_{2A} adenosine receptor antagonists in the therapy of Parkinson's disease. *Pharmacol. Ther.* **2011**, *132*, 280–299.

5 Fredholm, B. B.; IJzerman, A. P.; Jacobson, K. A.; Linden, J.; Müller, C. E. International Union of Basic and Clinical Pharmacology. LXXXI. Nomenclature and classification of adenosine receptors–an update. *Pharmacol. Rev.* **2011**, *63*, 1–34.

6 Svenningsson, P.; Le Moine, C.; Fisone, G.; Fredholm, B. B. Distribution, biochemistry and function of striatal adenosine A_{2A} receptors. *Prog. Neurobiol.* **1999**, *59,* 355−396.

7 a) Ferré, S.; Quiroz C.; Woods, A. S.; Cunha, R.; Popoli, P.; Ciruela, F.; Lluis, C.; Franco, R.; Azdad, K.; Schiffmann, S. N. An update on adenosine A_{2A}-dopamine D_2 receptor interactions. Implications for the function of G-protein coupled receptors. *Curr. Pharm. Des.* **2009**, *14*, 1468–1474. b) Ferré, S.; Fredholm, B. B.; Morelli, M.; Popoli, P.; Fuxe, K. Adenosine-dopamine receptor-receptor interactions as an integrative mechanism in the basal ganglia. *Trends Neurosci.* **1997**, *20*, 482–487.

8 a) Ferré, S.; Navarro, G.; Casadó, V.; Cortés, A.; Mallol, J.; Canela, E. I.; Lluís, C.; Franco, R. G protein-coupled receptor heteromers as new targets for drug development. *Prog. Mol. Biol. Transl. Sci.* **2010**, *91*, 41–52. b) Pollack, A. E.; Fink, J. S. Adenosine antagonists potentiate D_2 dopamine dependent activation of Fos in the striatopallidal pathway. *Neuroscience* **1995**, *68*, 721–728.

9 a) Lozano, A. M.; Lang, A. E.; Hutchison, W. D.; Dostrovsky, J. O. New developments in understanding the etiology of Parkinson's disease and in its treatment. *Curr. Opin. Neurobiol.* **1998**, *8*, 783–790. b) Müller, C. E.; Ferré, S. Blocking striatal adenosine A_{2A} receptors: a new strategy for basal ganglia disorders. *Recent Pat. CNS Drug Discov.* **2007**, *2*, 1–21.

10 a) Müller, C. E. A_{2A} Adenosine receptor antagonists – future drugs for Parkinson's disease? *Drugs Future* **2000**, *25*, 1043–1052. b) Müller, C. E.; Jacobson, K. A. Recent developments in adenosine receptor ligands and their potential as novel drugs. *Biochim. Biophys. Acta – Biomembranes* **2011**, 1290–1308. c) Baraldi, P. G.; Tabrizi, M. A.; Bovero, A.; Avitabile, B.; Preti, D.; Fruttarolo, F.; Romagnoli, R.; Varani, K.; Borea, P. A. Recent developments in the field of A_{2A} and A_3 adenosine receptor antagonists. *Eur. J. Med. Chem.* **2003**, *38*, 367–382. d) Baraldi, P. G.; Tabrizi, M. A.; Gessi, S.; Borea, P. A. Adenosine receptor antagonists: translating medicinal chemistry and pharmacology into clinical utility. *Chem. Rev.* **2008**, *108*, 238–263.

11 a) Salamone, J. D. Preladenant, a novel adenosine A_{2A} receptor antagonist for the potential treatment of parkinsonism and other disorders. *IDrugs.* **2010**, *13*, 723–731. b) Cristalli, G.; Müller, C. E.; Volpini, R. Recent developments in adenosine A_{2A} receptor ligands. *Handb. Exp. Pharmacol.* **2009**, *193*, 59–98.

12 Black, K. J.; Koller, J. M.; Campbell, M. C.; Gusnard, D. A.; Bandak, S. I. Quantification of indirect pathway inhibition by the adenosine A_{2A} antagonist SYN115 in Parkinson disease. *J. Neurosci.* **2010**, *30*, 16284–16292.

13 Gütschow, M.; Schlenk, M.; Gäb, J.; Paskaleva, M.; Alnouri, M. W.; Scolari, SW.; Iqbal, J.; Müller, C. E. Benzothiazinones: A novel class of adenosine receptor antagonists structurally unrelated to xanthine and adenine derivatives. *J. Med. Chem.* **2012**, *55*, 3331–3341.

14 a) Carlsson, J.; Yoo, L.; Gao, Z. G.; Irwin, J. J.; Shoichet, B. K.; Jacobson, K. A. Structure-based discovery of A_{2A} adenosine receptor ligands. *J. Med. Chem.* **2010**, *53*, 3748–3755. b) van der Horst, E.; van der Pijl, R.; Mulder-Krieger, T.; Bender A.; IJzerman A. P. Substructure-based virtual screening for adenosine A_{2A} receptor ligands. *ChemMedChem.* **2011**, *6*, 2302–2311.

15 a) Pisani, L.; Muncipinto, G.; Miscioscia, T. F.; Nicolotti, O.; Leonetti, F.; Catto, M. Caccia, C.; Salvati, P.; Soto-Otero, R.; Mendez-Alvarez, E.; Passeleu, C.; Carotti A. Discovery of a novel class of potent coumarin monoamine oxidase B inhibitors: development and biopharmacological profiling of 7-[(3-chlorobenzyl)oxy]-4-[(methylamino)methyl]-2*H*-chromen-2-one methanesulfonate (NW-1772) as a highly potent, selective, reversible, and orally active monoamine oxidase B inhibitor. *J. Med. Chem.* **2009**, *52*, 6685–6706. b) Maccioni, E.; Alcaro, S.; Cirilli, R.; Vigo, S.; Cardia, M. C.; Sanna, M. L.; Meleddu, R.; Yanez, M.; Costa, G.; Casu, L.; Matyus, P.; Distinto, S. 3-Acetyl-2,5-diaryl-2,3-dihydro-1,3,4-oxadiazoles: a new scaffold for the selective inhibition of monoamine oxidase B. *J. Med. Chem.* **2011**, *54*, 6394–6398. c) Gaspar, A., Silva, T.; Yáñez, M.; Vina, D.; Orallo, F.; Ortuso, F.; Uriarte, E.; Alcaro, S.; Borges, F. Chromone, a privileged scaffold for the development of monoamine oxidase inhibitors. *J. Med. Chem.* **2011**, *54*, 5165–5173.

16 a) Riederer, P.; Lachenmayer, L.; Laux, G. Clinical applications of MAO-inhibitors. *Curr. Med. Chem.* **2004**, *11*, 2033–2043. b) Youdim, M. B.; Bakhle, Y. S. Monoamine oxidase: isoforms and inhibitors in Parkinson's disease and depressive illness. *Br. J. Pharmacol.* **2006**, *147*, S287–S296.

17 Nicotra, A.; Pierucci, F.; Parvez, H.; Senatori, O. Monoamine oxidase expression during development and aging. *NeuroToxicology* **2004**, *25*, 155–165.

18 Sayre, L. M.; Perry, G.; Smith, M. A. Oxidative stress and neurotoxicity. *Chem. Res. Toxicol.* **2008**, *21*, 172–188.

19 a) Pålhagen, S.; Heinonen, E.; Hägglund, J. Selegiline slows the progression of the symptoms of Parkinson disease. *Neurology* **2006**, *66*, 1200–1206. b) Parkinson study group. A controlled,

randomized, delayed-start study of rasagiline in early Parkinson's disease. *Arch. Neurol.* **2004**, *61*, 561–566.

20 a) Schapira, A. H. V. Monoamine oxidase B inhibitors for the treatment of Parkinson's disease: a review of symptomatic and potential disease-modifying effects. *CNS Drugs* **2011**, *25*, 1061–1071. b) Schapira, A. H.; Stocchi, F.; Borgohain, R.; Onofrj, M.; Bhatt, M.; Lorenzana, P.; Lucini, V.; Giuliani, R.; Anand, R. Long-term efficacy and safety of safinamide as add-on therapy in early Parkinson's disease. *Eur. J. Neurol.* **2013**, 20, 271–280.

21 a) Pisani, L.; Catto, M.; Leonetti, F.; Nicolotti, O.; Stefanachi, A.; Campagna, F.; Carotti, A. Targeting monoamine oxidases with multipotent ligands: an emerging strategy in the search of new drugs against neurodegenerative diseases. *Curr. Med. Chem.* 2**011**, *18*, 4568–4587. b) Morphy, R.; Rankovic, Z. Designed multiple ligands. An emerging drug discovery paradigm. *J. Med. Chem.* **2005**, *48*, 6523–6543. c) Patyar, S.; Prakash, A.; Medhi, B. Dual inhibition: a novel promising pharmacological approach for different disease conditions. *J. Pharm. Pharmacol.* **2011**, *63*, 459–471. d) Elsinghorst, P. W.; Härtig, W.; Gündisch, D.; Mohr, K.; Tränkle, C.; Gütschow, M. A hydrazide linker strategy for heterobivalent compounds as ortho- and allosteric ligands of acetylcholine-binding proteins. *Curr. Top. Med. Chem.* **2011**, *11*, 2731–2748. e) Dunkel, P.; Gelain, A.; Barlocco, D.; Haider, N.; Gyires, K.; Sperlágh, B.; Magyar, K.; Maccioni, E.; Fadda, A., Mátyus, P. Semicarbazide-sensitive amine oxidase/vascular adhesion protein 1: recent developments concerning substrates and inhibitors of a promising therapeutic target. *Curr. Med. Chem.* **2008**, *15*, 1827–1839.

22 a) Weinreb, O.; Amit, T.; Bar-Am, O.; Youdim, M. B. Ladostigil: a novel multimodal neuroprotective drug with cholinesterase and brain-selective monoamine oxidase inhibitory activities for Alzheimer's disease treatment. *Curr. Drug Targets.* **2012**, *13*, 483–494. b) Youdim, M. B.; Fridkin, M.; Zheng, H. Bifunctional drug derivatives of MAO-B inhibitor rasagiline and iron chelator VK-28 as a more effective approach to treatment of brain ageing and ageing neurodegenerative diseases. *Mech. Ageing Dev.* **2005**, *126*, 317–326. c) Samadi, A.; de los Ríos, C.;

Bolea, I.; Chioua, M.; Iriepa, I.; Moraleda, I.; Bartolini, M.; Andrisano V.; Gálvez, E.; Valderas, C.; Unzeta, M.; Marco-Contelles, J. Multipotent MAO and cholinesterase inhibitors for the treatment of Alzheimer's disease: synthesis, pharmacological analysis and molecular modeling of heterocyclic substituted alkyl and cycloalkyl propargyl amine. *Eur. J. Med. Chem.* **2012**, *52*, 251–262. d) Bolea, I.; Juárez-Jiménez, J.; de Los Ríos, C.; Chioua, M.; Pouplana, R.; Luque, F. J.; Unzeta, M.; Marco-Contelles, J.; Samadi, A. Synthesis, biological evaluation, and molecular modeling of donepezil and *N*-[(5-(benzyloxy)-1-methyl-1*H*-indol-2-yl)methyl]-*N*-methylprop-2-yn-1-amine hybrids as new multipotent cholinesterase/monoamine oxidase inhibitors for the treatment of Alzheimer's disease. *J. Med. Chem.* **2011**, *54*, 8251–8270.

23 a) Chen, J. F.; Steyn, S.; Staal, R.; Petzer, J. P.; Xu, K.; Van der Schyf, C. J.; Castagnoli, K.; Sonsalla, P. K.; Castagnoli Jr., N.; Schwarzschild, M. A. 8-(3-Chlorostyryl)caffeine may attenuate MPTP neurotoxicity through dual actions of monoamine oxidase inhibition and A_{2A} receptor antagonism. *J. Biol. Chem.* **2002**, *277*, 36040–36044. b) Aguiar, L. M.; Macêdo, D. S.; Vasconcelos, S. M.; Oliveira, A. A.; de Sousa F. C.; Viana, G. S. CSC, an adenosine A(2A) receptor antagonist and MAO B inhibitor, reverses behavior, monoamine neurotransmission, and amino acid alterations in the 6-OHDA-lesioned rats. *Brain Res.* **2008**, *1191*, 192–199. c) Petzer, J. P.; Castagnoli, N. Jr.; Schwarzschild, M. A.; Chen, J. F.; Van der Schyf, C. J. Dual-target-directed drugs that block monoamine oxidase B and adenosine A_{2A} receptors for Parkinson's disease. *Neurotherapeutics* **2009**, *6*, 1 41–151.

24 a) Petzer, J. P.; Steyn, S.; Castagnoli, K. P., Chen, J. F., Schwarzschild, M. A., Van der Schyf, C. J., Castagnoli, N. Inhibition of monoamine oxidase B by selective adenosine A_{2A} receptor antagonists. *Bioorg. Med. Chem*. **2003**, *11*, 1299–1310. b) Pretorius, J.; Malan, S.; Castagnoli Jr., N.; Bergh, J. J.; Petzer J. P. Dual inhibition of monoamine oxidase B and antagonism of the adenosine A_{2A} receptor by (*E*,*E*)-8-(4-phenylbutadien-1-yl)caffeine analogues. *Bioorg. Med. Chem.* **2008**, *16*, 8676–8684. c) Rivara, S.; Piersanti, G.; Bartoccini, F.; Diamantini, G.; Pala, D.; Riccioni, T.; Stasi, M. A.; Cabri, W.; Borsini, F.; Mor, M.; Tarzia, G.; Minetti, P. Synthesis of (*E*)-8-(3-

chlorostyryl)caffeine analogues leading to 9-deazaxanthine derivatives as dual A_{2A} antagonists/MAO-B inhibitors. *J. Med. Chem.* **2013**, *56*, 1247–1261.

25 Müller, C. E.; Thorand, M.; Qurishi, R.; Diekmann, M.; Jacobson, K. A.; Padgett, W. L.; Daly, J. W. Imidazo[2,1-*i*]purin-5-ones and related tricyclic water-soluble purine derivatives: potent A_{2A}- and A_3-adenosine receptor antagonists. *J. Med. Chem.* **2002**, *45*, 3440–3450.

26 Vollmann, K.; Qurishi, R.; Hockemeyer, J.; Müller, C. E. Synthesis and properties of a new water-soluble prodrug of the adenosine A_{2A} receptor antagonist MSX-2. *Molecules* **2008**, *13*, 348–359.

27 a) Hockemeyer, J.; Joachim, C. B., Müller, C. E. Multigram-scale syntheses, stability, and photoreactions of A_{2A} adenosine receptor antagonists with 8-styrylxanthine structure: potential drugs for Parkinson's disease. *J. Org. Chem.* **2004**, *69*, 3308–3318. b) Müller, C. E.; Schobert, U.; Hipp, J.; Geis, U.; Frobenius, W.; Pawłowski, M. Configurationally stable analogs of 8-styrylxanthines as A_{2A}-adenosine receptor antagonists. *Eur. J. Med. Chem.* **1997**, *32*, 709–719. c) Nonaka, Y.; Shimada, J.; Nonaka, H.; Koike, N.; Aoki, N.; Kobayashi, H.; Kase, H.; Yamaguchi, K.; Suzuki, F. Photoisomerization of a potent and selective adenosine A_2 antagonist, (*E*)-1,3-dipropyl-8-(3,4-dimethoxystyryl)-7-methylxanthine. *J. Med. Chem.* **1993**, *36*, 3731–3733.

28 Leistner, S.; Gütschow, M.; Stach, J. 2-Amino-3,1-benzothiazin-4-ones: synthesis, Dimroth rearrangement to quinazolin-4(3*H*)-on-2(1*H*)-thiones, and MS/MS-fragmentation. *Arch. Pharm. (Weinheim, Ger.)* **1990**, *323*, 857–861.

29 Müller, C. E.; Hockemeyer, J.; Tzvetkov, N.; Burbiel, J. Preparation of 8-ethynyl-xanthine derivatives as selective A_{2A} receptor antagonists, PCT Int. Appl., 2008077557, 03 Jul 2008.

30 Travis, B. R.; Sivakumar, M.; Hollist, G. O.; Borhan, B. Facile oxidation of aldehydes to acids and esters with oxone. *Org. Lett.* **2003**, *5*, 1031–1034.

31 Neumann, U.; Gütschow, M. 3,1-Benzothiazin-4-ones and 3,1-benzoxazin-4-ones: highly different activities in chymotrypsin inactivation. *Bioorg. Chem.* **1995**, *23*, 72–88.

32 Scheiff, A. B.; Yerande, S. G.; El-Tayeb, A.; Li, W.; Inamdar, G. S.; Vasu, K. K.; Sudarsanam, V.; Müller, C. E. 2-Amino-5-benzoyl-4-phenylthiazoles: development of potent and selective adenosine A_1 receptor antagonists. *Bioorg. Med. Chem.* **2010**, *18*, 2195–2203.

33 Müller, C. E.; Jacobson, K. A. Xanthines as Adenosine Receptor antagonists. In *Methylxanthines. Handbook of Experimental Pharmacology 200, 1st ed.;* Fredholm, B. B., Ed.; Springer-Verlag Berlin Heidelberg, 2011; pp 151–199.

34 Weiss, S. M.; Benwell, K.; Cliffe, I. A.; Gillespie, R. J.; Knight, A. R.; Lerpiniere, J.; Misra, A.; Pratt, R. M.; Revell, D.; Upton, R.; Dourish, C. T. Discovery of nonxanthine adenosine A_{2A} receptor antagonists for the treatment of Parkinson's disease. *Neurology* **2003**, *61*, 101–106.

35 Jacobson, K. A.; Gallo-Rodriguez, C.; Melman, N.; Fischer, B.; Maillard, M.; van Bergen, A.; van Galen, P. J.; Karton, Y. Structure–activity relationships of 8-styrylxanthines as A_2-selective adenosine antagonists. *J. Med. Chem.* **1993**, *36*, 1333–1342.

36 Sterling, J.; Herzig, Y.; Goren, T.; Finkelstein, N.; Lerner, D, Goldenberg, W.; Miskolczi, I.; Molnar, S.; Rantal, F.; Tamas, T.; Toth, G.; Zagyva, A.; Zekany, A.; Finberg, J.; Lavian, G.; Gross, A.; Friedman, R.; Razin, M.; Huang, W.; Krais, B.; Chorev, M.; Youdim, M. B.; Weinstock, M. Novel dual inhibitors of AChE and MAO derived from hydroxy aminoindan and phenethylamine as potential treatment for Alzheimer's disease. *J. Med. Chem.* **2002**, *45*, 5260–5279.

37 Chimenti, F.; Secci, D.; Bolasco, A.; Chimenti, P.; Granese, A.; Carradori, S.; Yáñez, M.; Orallo, F.; Sanna, M. L.; Gallinella, B.; Cirilli, R. Synthesis, stereochemical separation, and biological evaluation of selective inhibitors of human MAO-B: 1-(4-Arylthiazol-2-yl)-2-(3-methylcyclohexylidene)hydrazines. *J. Med. Chem.* **2010**, *53*, 6516–6520.

38 Novaroli, L.; Daina, A.; Favre, E.; Bravo, J.; Carotti, A.; Leonetti, F.; Catto, M.; Carrupt, P. A.; Reist, M. Impact of species-dependent differences on screening, design, and development of MAO B inhibitors. *J. Med. Chem.* **2006**, *49*, 6264–6272.

39 Müller, C. E.; Maurinsh, J.; Sauer, R. Binding of [^{3}H]MSX-2 (3-(3-hydroxypropyl)-7-methyl-8-(*m*-methoxystyryl)-1-propargylxanthine) to rat striatal membranes - a new, selective antagonist radioligand for A_{2A} adenosine receptors. *Eur. J. Pharm. Sci.* **2000**, *10*, 259–265.

40 Borrmann, T.; Hinz, S.; Bertarelli, D. C.; Li, W.; Florin, N. C.; Scheiff, A. B.; Müller, C. E. 1-Alkyl-8-(piperazine-1-sulfonyl)-phenylxanthines: development and characterization of adenosine A_{2B} receptor antagonists and a new radioligand with subnanomolar affinity and subtype specificity. *J. Med. Chem.* **2009**, *52*, 3994–4006.

41 Müller, C. E.; Diekmann, M.; Thorand, M.; Ozola, V. [^{3}H]8-Ethyl-4-methyl-2-phenyl-(8R)-4,5,7,8-tetrahydro-1H-imidazo[2,1-*i*]-purin-5-one ([^{3}H]PSB-11), a novel high-affinity antagonist radioligand for human A_3 adenosine receptors. *Bioorg. Med. Chem. Lett.* **2002**, *12*, 501–503.

42 Bulicz, J.; Bertarelli, D. C.; Baumert, D.; Fülle, F.; Müller, C. E.; Heber, D. Synthesis and pharmacology of pyrido[2,3-*d*]-pyrimidinediones bearing polar substituents as adenosine receptor antagonists. *Bioorg. Med. Chem*. **2006**, *14*, 2837–2849.

43 Klotz, K. N.; Lohse, M. J.; Schwabe, U.; Cristalli, G.; Vittori, S.; Grifantini, M. 2-Chloro-N^6-[^{3}H]cyclopentyladenosine ([^{3}H]CCPA) - a high affinity agonist radioligand for A_1 adenosine receptors. *Naunyn-Schmiedeberg's Arch. Pharmacol.* **1989**, *340*, 679–683.

44 Yan, L.; Bertarelli, D. C.; Hayallah, A. M.; Meyer, H.; Klotz, K.. N.; Müller, C. E. A new synthesis of sulfonamides by aminolysis of pnitrophenylsulfonates yielding potent and selective adenosine A_{2B} receptor antagonists. *J. Med. Chem.* **2006**, *49*, 4384−4391.

45 Schumacher, B.; Scholle, S.; Holzl, J.; Khudeir, N.; Hess, S.; Müller, C. E. Lignans isolated from valerian: identification and characterization of a new olivil derivative with partial agonistic activity at A_1 adenosine receptors. *J. Nat. Prod.* **2002**, *65*, 1479−1485.

46 a) Schiedel, A. C.; Hinz, S.; Thimm, D.; Sherbiny, F.; Borrmann, T.; Maass, A.; Müller C. E. The four cysteine residues in the second extracellular loop of the human adenosine A_{2B} receptor: role in ligand binding and receptor function. *Biochem. Pharmacol.* **2011**, *82*, 389−399. b) Nordstedt, C.;

Fredholm, B. B. A modification of a protein-binding method for rapid quantification of cAMP in cell-culture supernatants and body fluid. *Anal. Biochem.* **1990**, *189*, 231−234.

Table of Contents Graphic